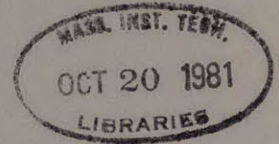


TJ778  
.M41  
.G24  
no. 161



AERO



An Experimental Investigation of Stator  
Hub Treatment in an Axial Flow  
Compressor

by  
Mark E. Prell

GT&PDL Report No. 161

July 1981



**GAS TURBINE & PLASMA DYNAMICS LABORATORY**  
MASSACHUSETTS INSTITUTE OF TECHNOLOGY  
CAMBRIDGE, MASSACHUSETTS

An Experimental Investigation of Stator  
Hub Treatment in an Axial Flow  
Compressor

by  
Mark E. Prell

GT&PDL Report No. 161      July 1981

This research, carried out in the Gas Turbine  
and Plasma Dynamics Laboratory, MIT, was  
supported by the Air Force Office of Scientific  
Research, Contract Number F49620-78-C-0084,  
Dr. J. D. Wilson, Program Manager.

## ABSTRACT

An experiment was carried out to examine the effects, on stator stall margin and performance, of a slotted hub treatment rotating beneath the stator of an axial flow compressor. The compressor was run with this hub treatment and the results compared to those taken with a smooth rotating hub. It was determined that, for the configuration tested, the hub treatment was ineffective in the improvement of stall margin but resulted in a measurably higher static pressure rise across the stator and a significant decrease in flow deviation and blockage in the stator midspan region. Although it is the hub section of the stator that sets the stall limit in this configuration, measurements of the stator exit flow field indicated that the type of stall that is occurring is a blade stall rather than a pure wall stall. Absence of a wall stall is thus seen as a key possibility for the lack of stall margin improvement.

**0743123**

## ACKNOWLEDGMENTS

The author is indebted to many members of the Gas Turbine Laboratory staff for their valuable assistance in the design, construction and operation of this experiment. In particular I wish to thank Professor E. M. Greitzer for his guidance and encouragement in all phases of this project, and to Dr. C. S. Tan for designing the computer hardware and software. Special thanks is extended to J. Marksteiner and G. Paluccio for their craftsmanship and dedication in the mechanical aspect.

This work was supported by the Air Force Office of Scientific Research, Contract Number F49620-78-C-0084, Dr. J. D. Wilson, Program Manager.

## TABLE OF CONTENTS

	Page
ABSTRACT	2
ACKNOWLEDGMENTS	3
LIST OF FIGURES	6
NOMENCLATURE	9
CHAPTER 1 INTRODUCTORY REMARKS	11
1.1 INTRODUCTION	11
1.2 LITERATURE SURVEY	13
CHAPTER 2 DESCRIPTION OF EXPERIMENT	20
2.1 EXPERIMENT DESIGN	20
2.2 EXPERIMENTAL FACILITY	22
2.3 TREATMENT DESIGN	24
2.4 INSTRUMENTATION	25
2.5 DATA REDUCTION	27
CHAPTER 3 EXPERIMENTAL RESULTS	30
3.1 EFFECT OF HUB TREATMENT ON STATOR STALL	30
3.2 COMPRESSOR PERFORMANCE	35
3.3 ANALYSIS USING THE AXISYMMETRIC DESIGN PROGRAM	40
3.4 DIAGNOSTIC TESTS	42
CHAPTER 4 CONCLUSIONS AND RECOMMENDATIONS	45
4.1 SUMMARY AND CONCLUSIONS	45
4.2 RECOMMENDATIONS	47
REFERENCES	49
FIGURES	51

## TABLE OF CONTENTS (CONTINUED)

	Page
APPENDIX A	80
APPENDIX B	83
APPENDIX C	88

## LIST OF FIGURES

## Figure No

1. D-Factor Design Profiles
2.  $\Delta P/q$  Design Profiles
3. Compressor Cross Section
4. Hub Treatment Geometry
5. Rotor/Hub Treatment Assembly
6. Instrumentation Layout
7. Overall Total to Static Pressure Rise Characteristic
8. Stator Static Pressure Rise Characteristic
9. Rotor Total Pressure Rise Characteristic
10. Hot Wire Signal at Treated Stator Discharge
11. Hot Wire Signal at Untreated Stator Discharge
12. Hot Wire Signal at Treated Stator Discharge, Stall Point
13. Hot Wire Signal at Untreated Stator Discharge, Stall Point
14. Hot Wire Signal at Treated Stator Inlet and Discharge,  
Stall Point
15. Hot Wire Signal at Untreated Stator Inlet and Discharge,  
Stall Point
16. FFT Spectrum of Stator Hub Exit, Stall
17. FFT Spectrum of Stator Hub Exit, No Stall
18. Inlet Total Pressure Profile vs. Design
19. IGV Exit Air Angle Profile vs. Design
20. Rotor Exit Total Pressure Profile vs. Design, Stall Point
21. Rotor Exit Air Angle Profile vs. Design, Stall Point
22. Untreated Stator Exit Air Angle Profile vs. Carter's  
Rule, Stall Point

## LIST OF FIGURES (CONTINUED)

## Figure No

23. Treated Hub: Rotor and Stator Total Pressure Profile, Stall Point
24. Untreated Hub: Rotor and Stator Total Pressure Profile, Stall Point
25. Stator Exit Air Angle Profile at Stall Point, Treated vs. Untreated
26. Untreated Hub: Stator Wake Total Pressure Traverse, Stall Point vs.  $\phi_{MAX}$
27. Untreated Hub: Stator Wake Deviation Angle Traverse, Stall Point vs.  $\phi_{MAX}$
28. Treated Hub: Stator Wake Total Pressure Traverse at Stall Point
29. Untreated Hub: Stator Wake Total Pressure Traverse at Stall Point
30. Treated Hub: Stator Wake Deviation Angle Traverse at Stall Point
31. Untreated Hub: Stator Wake Deviation Angle Traverse at Stall Point
32. Untreated Hub: Rotor and Stator D-Factor Profile at Stall (Based on Axisymmetric Calculation)
33. Untreated Hub: Rotor and Stator  $\Delta P/q$  Profiles at Stall (Based on Axisymmetric Calculation)
34. Stator D-Factor Profile at Stall, Treated vs. Untreated (Based on Axisymmetric Calculation)



## LIST OF FIGURES (CONTINUED)

## Figure No

35. Stator  $\Delta P/q$  Profiles at Stall, Treated vs. Untreated  
(Based on Axisymmetric Calculation)
36. Stator Axial Velocity Profile at Stall, Treated vs.  
Untreated (Based on Axisymmetric Calculation)
37. Stator Relative Total Pressure Loss Coefficient Profile  
at Stall, Treated vs. Untreated (Based on Axisymmetric  
Calculation)
38. Untreated Stator Exit Air Angle Profiles: Stall Point  
and Near Stall Point

## NOMENCLATURE

C	absolute velocity
$C_u$	tangential velocity
$C_x$	axial velocity
D-Factor	diffusion factor, $1 - (W_2/W_1) + (\Delta W_u/2\sigma W_1)$
IM	radial immersion fraction, $1 - \frac{R_{tip} - R}{R_{tip} - R_{hub}}$
$P_s$	static pressure
$\Delta P_s$	static pressure difference
$P_t$	total pressure
$\Delta P_t$	total pressure difference
Q	relative dynamic pressure at blade inlet, $1/2\rho W_1^2$
R	radial coordinate
U	mean wheel speed
W	relative velocity
x	axial coordinate
$\alpha$	absolute air angle measured from axial direction
$\beta$	blade relative air angle measured from axial direction
$\sigma$	solidity, chord/gap
$\phi$	flow coefficient, $C_x/u$
$\theta$	tangential coordinate
$\rho$	density
$\bar{\omega}$	relative total pressure loss coefficient, $\Delta P_{trel}/1/2\rho W_1^2$
$\delta$	deviation angle

## Subscripts:

1	blade inlet
2	blade exit
rel	blade relative reference frame
t	measured on casing
in	measured at compressor inlet
ex	measured at compressor discharge

## CHAPTER 1

## INTRODUCTORY REMARKS

## 1.1 INTRODUCTION

It has been known for over a decade that the application of slots or grooves over the rotor tips in the casing of an axial flow compressor can lead to a significant improvement in the stall margin. Previous studies have indicated that a substantial reduction of the endwall boundary layer blockage in the rotor tip region, and an interchange of fluid between the treatment and blade passage, are associated with the operation of casing treatment. These effects are apparently due to the relative motion of the treatment and blades, and it is thus natural to ask whether a rotating treatment below a row of stator blades would also be effective in improving the stall margin of the stator. However, very little research has been done on the subject of hub treatment, and to date it has not been conclusively demonstrated whether it is an effective means of inhibiting stator hub stall in an axial flow compressor. This has left a gap in our knowledge of the treatment phenomena, and further research is required in this area to enhance our understanding of the effects of treatment on compressor stall. A successful demonstration of hub treatment would also set the stage for experiments which could analyze the effect of treatment on the blade relative flow in the absolute frame, thus eliminating the need for rotating frame instrumentation, and would provide a different perspective from which to view the overall phenomenon.

In the present study the rotor of a single stage axial flow compressor was fitted with an extended cylindrical hub which rotated under the tips of the cantilevered stator vanes. Experiments were run with a "baseline" smooth cylinder, and with a treated hub. The treatment employed consists of axially oriented slots covering the middle 80% of the stator chord, skewed at an angle of  $60^\circ$  to the radial direction. This axial skewed treatment was chosen for its proven effectiveness in the casing treatment application.

In the design of the experiment several aerodynamic conditions are considered which can influence the effect of the treatment on stall margin. First it is desired that the compressor be stall limited at the stator hub. In this case the rotor is very lightly loaded at the stall point and acts only as a "flow generator" for the stator. The rotor loading is also tip biased producing locally high loading at the stator hub. The treatment effectiveness may also depend upon whether a blade or wall stall is produced, as it has been established by Greitzer et al. (Ref. 1) that for some geometries casing treatment may not be effective in the presence of a dominant blade stall. Since it can be difficult to accurately predict whether a given geometry will produce a blade stall or wall stall, this question must be examined experimentally.

The purpose of this experiment is to examine the effect of hub treatment on the stall margin and performance of a hub critical stator. This thesis presents the design of the

treatment and stage geometry as well as the results of these experiments.

## 1.2 LITERATURE SURVEY

A thorough review of the literature has recently been given by Smith (Ref. 2) and this survey will therefore cover only some of the previous research that is directly relevant to this study. Part A of this section will describe casing treatment research. Hub treatment is covered in Part B.

### A) Casing Treatment

One of the first attempts at understanding the mechanism characterizing casing treatment stall margin improvement was an experiment by Prince, Wisler and Hilvers, on the General Electric Co. low speed research compressor (Ref. 3). In this study the stall margin of a tip critical stage was tested with solid casing, circumferential groove, blade angle slots, and axial skewed slot casing treatments. All treatments were found to improve stall margin, with the axial skewed and blade angle slot treatments showing the greatest gains. Flow visualization of the slot flows with yarn tufts showed a predominant flow out of the blade angle treatment cavities near the leading edge. Hot wire measurement of the slot flow confirmed the existence of strong radial velocities near the treatment, but could not establish the sense of the flow, i.e., entering or leaving. Spanwise traverses showed that the tip annulus boundary layers were thinned at rotor exit in the presence of the slot treatments.

Takata and Tsukuda (Ref. 4) tested five different treatments and varied the tip clearance and slot depth. In general their results confirmed the improvements seen by Prince et al., with the axial skewed slot treatment showing the highest improvement (20%\*), and the circumferential groove treatment the lowest (4%). One treatment, the reversed axial skewed slots actually showed a deficit in stall margin (-14%). In this treatment, the flow leaving the slots had a swirl component in the direction of blade rotation. It would thus appear that the orientation in which the flow left the slots had a strong effect on treatment operation. It was also found that variation of slot depth, and the presence of a back chamber, or plenum, with the axial skewed slots had little or no effect on the stall margin improvement, and that increase of tip clearance (from .3% to 1.3% span), did not diminish the effect of the treatment. On the contrary, the largest improvement of all was seen with the axial skewed treatment having the highest tip clearance. Spanwise traverses of the inlet flow angle just before stall showed that the treatment allowed the rotor to operate at 5° higher incidence. It was also confirmed that the thinning of the casing endwall boundary layer as reported by Prince was a characteristic of the casing treatment and was most notable with the axial skewed slots.

---

\* Percent Improvement =  $1 - \frac{\text{Treated Stall Flow}}{\text{Untreated Stall Flow}}$

Hot wire measurements within the axial skewed slot revealed a fluctuating flow at the blade passing frequency. It was determined that the flow entered the slot near the blade trailing edge and emerged near the leading edge, thus indicating a recirculating flow pattern in the grooves. The slot flows were found to have a jet like character, pulsing regularly at blade passing frequency. The jet velocities were comparable to the mean flow in magnitude.

Greitzer, Nikkanen, Haddad, Mazzawy, and Joslyn (Ref. 1) tested an axial skewed slot configuration with two different compressor rotor geometries. The first was designed so that a blade stall would be encountered at the rotor tip. This type of stall is produced by separation of the blade suction surface boundary layer and is characterized by large rotor wakes. In the second case a wall stall was produced on the casing endwall above the rotor tips by doubling the solidity of the first experiment and thus inhibiting blade stall. In the wall stall it is the flow blockage of the endwall boundary layer which is viewed as initiating stall and the blade wakes are small compared to the blade stall case. This experiment showed a substantial reduction in stalling flow coefficient when treatment was used for the high solidity (wall stall) configuration (14%), but a negligible change for the low solidity (blade stall) configuration, thus indicating that casing treatment is most effective in treating wall stall as opposed to blade stall. Rotating frame measurements downstream of the rotor also confirmed the reduction in endwall



blockage due to treatment, observed in the previous studies, and it was suggested that the stall improvement observed is due to this blockage reduction.

The most recent and thorough study of the treatment mechanism was done by Smith at the University of Cambridge (Ref. 2). Smith measured the flow field in axial skewed slots via hot wire anemometry and a traversing slide mechanism, and obtained relative frame measurements of pressure, velocity and flow direction via a rotating traverse mechanism. These results clearly show the previously mentioned recirculating flow pattern in the endwall/treatment region, and show the rotor operating at significantly higher incidence angles at stall with treatment, compared to the solid wall case. Smith postulates that for the configuration tested, stall is initiated by the flow blockage due to a large area of low relative total pressure on the casing endwall near the pressure surface of the rotor, and the treatment is effective in the elimination of this blockage. The improvement mechanism suggested is that the treatment reduces the blockage due to accumulation of low energy fluid on the casing endwall as previously suggested by Greitzer et al. (Ref. 1).

#### B. Hub Treatment

Comparatively little work has been done using a hub treatment rotating below the tips of a stationary row of blades. One study of this subject was done on the General Electric Co. low speed research compressor by Wisler

and Hilvers (Ref. 5). Two types of treatment found to be effective in the casing application (circumferential groove and radial blade angle slots) were tested in a two stage hub critical compressor with neither treatment showing a noticeable improvement in stall margin. However, the two stage geometry complicated the isolation of the stall limiting section, and this study did not cite conclusive evidence that the stall observed was due to the stator only. On the contrary, the analysis seemed to indicate a rotor hub stall. For the geometry tested the stage reactions were fairly high which would also tend to support this idea. Thus it is possible that the negative result was not due to the ineffectiveness of the hub treatment per se, but to the absence of a limiting stator hub, a condition required for stall margin improvement.

Takata and Tsukuda (Ref. 4) tested the effect of treatment on the vane relative total pressure distribution using a rotating hub treatment and stator. Although this experiment did not examine the question of stall margin improvement, it did show a positive result in that the endwall boundary layer blockage in the treatment vicinity was effectively reduced in a manner similar to that observed in casing treatment studies (Refs. 1-4).

One other interesting investigation of stall margin improvement of a stationary row of blades via a rotating treatment was done by Jansen, Carter, and Swarden (Ref. 6) on the vaned diffuser of a centrifugal compressor. A skewed

treatment similar to the short axial skewed slot casing treatment configuration, was applied to the impeller rim such that the treatment slots rotated under the forward portion of the diffuser vanes. The treatment application resulted in a significant increase in the stall margin (approximately 7%), and a large increase in the maximum flow. Thus it would seem that a substantial reduction in the flow blockage of the vaned diffuser, similar to that observed in the casing treatment studies can be attributed to the treatment.

One additional study which deserves mention in this section was conducted by Greitzer and Nikkanen and is reported by Mikolajczak and Pfeffer (Ref. 11). In this work an experiment was run in which the flow through a cantilevered cascade of vanes in a water tunnel was observed with a moving belt employed as the endwall beneath the cantilevered tips. This rig was tested with smooth, rough and treated belts, and compared to the stationary belt case. It was reported that near the moving wall a layer of fluid is "dragged" along at wall speed in the direction of belt motion and thus entrains fluid particles from the suction surface of the vane. Thus low energy fluid in the suction surface boundary layer is removed by a secondary flow induced by the moving endwall. This results in radial migration of the suction surface boundary layer fluid towards the moving endwall along the vane surface. When the boundary layer fluid reaches the end-wall region it is then swept across to the adjacent blade pressure surface where it can roll up in a vortex. The

intensity and radial extent of this flow was proportional to belt roughness, and was strongest with the treated belt.

As stated, there have also been many other investigations of this type. For a more extensive list of these, one can see Ref. 1 or Ref. 2 and we will not discuss the previous investigations further.

In the next section we will consider the design of the experiment and treatment and describe the experimental facility.

## CHAPTER 2

### DESCRIPTION OF EXPERIMENT

#### 2.1 EXPERIMENT DESIGN

It is fundamental in the design of this experiment to ensure that the stator hub endwall is stall limiting. The design used is aimed at having rotor loading very low at the stator stall point so that the rotor acts only as a "flow generator" for the stator. Thus, in choosing the blade setting angles, it is desired that the rotor has a high stagger angle relative to the stator and that stage reaction be low. The requirement of high stator hub loading can be satisfied by using a rotor blade with very low twist. This creates only a small static pressure rise across the rotor hub relative to the tip which in turn loads the stator hub. (It was fortunate that this requirement allowed the use of existing blades in which the rotor twist was only  $9.5^\circ$ ). In selection of the blade setting angles necessary for this series of tests it was also desired to have the stator discharge static pressure above ambient pressure at a flow somewhat above the stall point, so that the compressor would have adequate stable flow range.

The actual blade setting angles and radial load profiles were calculated using an axisymmetric compressor design program (Ref. 7) which had been matched to data taken previously on this compressor by Gopalakishnan (Ref. 8). The data match was accomplished by first determining an empirical relation of the departure of measured blade relative air angles from Carter's rule (Ref. 9), or "x-factor", vs. radius ratio. Secondly it

was assumed that radial profiles of relative total pressure loss coefficient ( $\bar{\omega}$ ) can be represented by an empirical relation of  $\bar{\omega}$  and D-factor, and a radial loss multiplier to account for the endwall boundary layers. The D-factor relation used is similar to that suggested by Lieblien (Ref. 10) and the endwall multiplier was determined from the total pressure profiles measured by Gopalakrishnan. This technique has been used by the author previously in compressor design work and found to give satisfactory results.

Once the data was matched, the relations were applied to the present blading geometry to determine the air angles and loss profiles for various combinations of rotor and stator stagger at a flow coefficient near the stall point. Although an accurate prediction of the actual stall point is very difficult, it is desired to compare the various cases at a flow coefficient near stall. For this purpose the assumption was made that a stall point had been reached when the D-factor or  $\Delta P/q$  exceeded a value of .6 at the streamline corresponding to approximately 90% immersion.\* Using this "stall criterion" a reasonable approximation of the stall point aerodynamics, suitable for our comparative purposes can be obtained. The optimum blade angles were then selected by comparing the computer runs and choosing the combination which best satisfied the design criteria.

---

\* % Immersion defined as  $1 - \frac{R_{tip} - R}{R_{tip} - R_{hub}}$

The resulting design is described in detail in section 2.2. The computer solution estimated that the stage reaction would be approximately .5 and the resulting D-factor and  $\Delta P/q$  profiles showed a very favorable stator hub load bias and rotor/stator load split as shown in Figs. 1 and 2. The maximum D-factor and  $\Delta P/q$  both occurred at the stator hub endwall, and had values of .6 and .52 respectively at the 90% immersion streamline. It is of course desirable to have a  $\Delta P/q$  as high as possible (relative to D-factor) at the stator hub since this condition increases the likelihood of wall stall. However, the calculations showed that a further increase in  $\Delta P/q$  could only be achieved by an increase in stator solidity. It was therefore decided to run this experiment with the existing blades and resolve the question of blade or wall stall experimentally.

## 2.2 EXPERIMENTAL FACILITY

The experiment was conducted on a single stage research compressor driven by a variable speed D.C. motor. The compressor was equipped with inlet guide vane, a discharge diffuser/valve, and a circumferentially traversing outer casing. The compressor was modified for casing treatment as well as hub treatment, as it is intended to be a vehicle for the study of both treatments. A cross sectional schematic of the compressor showing blading and treatment locations is given in Fig. 3.

Both rotor and stator have a constant chord of 38 mm,

an aspect ratio of 1.91, and a nominal solidity at midspan of 1.0. The IGV has a radially constant solidity of 1.0 and a chord of 38 mm at midspan. The rotor and stator are each 30° camber, and the IGV designed for approximately 20° pre-swirl. Further details of the flowpath are summarized below in Table I.

TABLE I. Flowpath Geometry

	<u>Rotor</u>	<u>Stator</u>
Hub diameter	444 mm	444 mm
Casing diameter	597 mm	597 mm
Number of blades	44	45
Chord	38 mm	38 mm
Solidity at midspan	1.0	1.0
Aspect ratio	1.91	1.91
Camber	30°	30°
O.D. stagger angle	49.5°	20°
Midspan stagger angle	44.7°	22.5°
I.D. stagger angle	40°	25°
Blade clearance	.76 mm	.76 mm

Most of the measurements were taken at 2800 RPM for both experiments; however runs were also made at 3500 RPM to check Reynolds number dependence. The Reynolds number based on blade chord at the stator hub was nominally  $1.5 \times 10^5$  at the stall point at 2800 RPM. Both rotor and



stator tip clearances were the same for the two experiments.

### 2.3 TREATMENT DESIGN

The hub treatment consists of axial slots skewed at a  $60^\circ$  angle to the radial direction, which rotate under the middle 80% of the stator tip chord. The slot spacing is such that the open or slotted area is twice that of the solid or land area. The slot aspect ratio (axial length/tangential width) is 2.0, and the radial depth is 30% of the axial length. The actual dimensions and treatment geometry are shown in Fig. 4.

The treated and smooth hub cylinders were cut from a solid billet of aluminum and machined to tolerance. The cylinders were bolted to the aft rotor disk, which was also constructed of aluminum. Clearance was provided in the disk bolt holes, being slotted such the the cylinder might expand radially relative to the disk under centrifugal load without creating high shear stresses on the bolts. The cylinder/disk assembly and dimensions are shown in Fig. 5, and the casing treatment and hub cylinder drawings are given in Appendix A. It should be noted that the axial spacing between rotor and stator is quite wide, (approximately 4 axial chord lengths). This condition is advantageous in this experiment in that it is desired to "decouple" the rotor and stator aerodynamics as much as possible.

The hub treatment was constructed by machining a wide circumferential groove in the cylinder and glueing pre-

machined plexiglass plates into the groove in a plane axially oriented and skewed  $60^\circ$  to the radial direction. The cylinder groove and plexiglass plates were cut with a slight dovetail to help anchor the plates under centrifugal force.

The compressor was modified for casing treatment by the insertion of a 76 mm long casing segment above the rotor tips in which the casing treatment was installed. The casing treatment chosen was also the axial-skewed design, and the treatment geometry and construction was identical to the hub treatment.

#### 2.4 INSTRUMENTATION

The pressure instrumentation consists of 20 total pressure "kiel" probes and 24 hub and casing static taps. It was located at five axial stations as shown in Fig. 6. At station 1 located 456 mm (6.5 spans) downstream of the inlet plane and 4 blade chords (2.5 spans) upstream of the IGV, there were 8 kiel probes mounted at the midspan and 4 casing wall statics. At station 2, 1 chord upstream of the IGV there were 4 wall statics on both casing and hub. Station 3 was located 1 chord downstream of the IGV and included 4 wall static taps on both casing and hub; however these taps were not used in this experiment. At station 4, 1.7 chords downstream of the rotor, there were 4 casing wall statics and 8 kiel probes. Single kiels at the midspan were mounted at the  $5^\circ$  and  $185^\circ$  circumferential positions while at the  $95^\circ$  and  $275^\circ$

positions there were 3 kiels mounted at centers of equal annulus area (hub, pitch, tip). Finally at station 5, 1 chord downstream of the stator, there were 4 wall statics on both casing and hub as well as 4 pitch mounted kiels. All five stations were equipped with a radial traverse port, and the casings at stations 2, 3 and 5 could rotate providing circumferential traverse capability at these locations.

The acquisition of the pressure data was done by a 48 channel scanivalve pressure scanner operated by a digital minicomputer. The computer/scanivalve logic interface consists of a digital circuit enabling the computer to read the channel number and step the valve, and an analog/digital converter which enabled the computer to read and store the transducer output signal. The A/D converter had a resolution of .05% and the overall pressure transducer error was less than .06% full scale. The uncertainty in the total pressure data is then .08% of full scale which corresponds to .4% of the total inlet dynamic head at the 2800 RPM stall point. A block diagram of the computer/scanivalve arrangement, and source listings of the data acquisition software are presented in Appendix B.

A radial traverse mechanism was used to determine radial profiles of total pressure and flow angle at all five measurement stations. The radial traverses behind the stator were taken at the mid gap location. As previously mentioned the rotating casing at station 5 enabled the determination of circumferential profiles of the stator wakes at various radial immersions. A three hole wedge probe of hole diameter .25 mm capable of sensing

total pressure and flow angle was used for the traverses.

A hot wire anemometer was used to gather dynamic data ahead of and behind the stator and to enable accurate determination of the stall point. The hot wire output was filtered to pass those frequencies between 10 and 200 Hz, thus concentrating the attention on the low frequencies associated with rotating stall and excluding those frequencies associated with the passage of the treatment slots or rotor wakes. The anemometer output was recorded on an oscillograph recorder, and digitized and stored by the computer. The digitized data was resolved in the frequency domain by a fast Fourier transform program. Source listings of the dynamic data acquisition and reduction software are presented in Appendix C.

The compressor speed was set and measured by a strobe tachometer which was accurate to 5 RPM or .18% of the nominal operating speed.

## 2.5 DATA REDUCTION

After several preliminary runs, it was determined that the most reliable and repetitive indication of flow rate was the average of the four casing statics at station 1. Radial traverses at this station indicated that the flow was essentially parallel with only small amplitude circumferential total pressure nonuniformities, and thus the measurement of static pressure at the casing should be representative of the entire annulus. The total pressure profile at this

station (see Fig. 16) was then integrated to obtain the mass flow rate.

The compressor speedline characteristic for the rotor was determined from the average of the 6 hub, pitch, and tip kiel total pressures, the overall total-to-static characteristic from the average of the 8 hub and casing wall statics at station 5, and the stator static pressure rise characteristic from the difference in the averages of the casing wall statics at stations 4 and 5.

In this thesis all pressure parameters except the circumferential stator traverse data were normalized by division by  $1/2 \rho U^2$ . The stator wake total pressure surveys are presented as the loss in total pressure across the stator divided by  $1/2 \rho C_1^2$  where  $C_1$  is defined as the absolute velocity at stator inlet at the radial position of the traverse.

It should be mentioned at this time that several data points were repeated because of oil contamination of the compressor blading and flowpath. The source was a leaking oil seal in the compressor drive bearing. This allowed the escape of oil mist into the air ingested by the compressor. This condition resulted in fouling of the blades and probes severe enough to significantly (>1%) affect the measured compressor performance in just three hours running time. However once the problem was identified, the compressor was carefully cleaned at regular intervals. In particular, special care was taken to ensure that comparative tests were

always run in a fully clean condition.

## CHAPTER 3

### EXPERIMENTAL RESULTS

In this section the results and analysis of the results will be presented. We will examine the effect of the treatment on stall margin and compressor speedline characteristics, discuss the stall and its source, compare the treated and untreated traverse data, and finally discuss the analysis of these results using the axisymmetric design program described in section 2.1.

#### 3.1 EFFECT OF HUB TREATMENT ON STATOR STALL

The application of hub treatment to the compressor described above resulted in a reduction of the stalling flow coefficient of only 1% and an increase in the stator static pressure rise characteristic of approximately 5% at the stall point. Since the experimental error is also on the order of 1% (see section 2.4), the improvement in stall flow due to treatment can be considered negligible. A comparison of the overall total to static pressure rise characteristic  $[(P_{S_{ex}} - P_{T_{in}})/1/2 \rho U^2]$  vs.  $(C_x/U)$  for both cases is shown in Fig. 7. The stall points are also indicated here and are at  $C_x/U \sim .53$  and  $.52$  for the untreated and treated cases respectively. Here we have defined "stall point" as being the maximum value of  $C_x/U$  at which stall is observed. Comparison of the data in Fig. 7 suggests a small but consistent increase in the static pressure level at the stator discharge for the treated case. Perhaps a more

meaningful way of looking at this trend is to examine the stator static pressure rise characteristics as determined from the casing wall static taps just ahead of and just behind the stator, as shown in Fig. 8. Here the increase in static pressure rise across the stator due to the hub treatment is evident at all flow coefficients tested and is approximately 5% of the static pressure rise of the stator with the untreated hub. The application of hub treatment has thus resulted in a small but measurable change in the stator aerodynamics.

A comparison of the rotor total pressure characteristic is given in Fig. 9. As expected there are no large differences in the rotor performance of the treated and untreated cases, and the negative slope of the characteristic indicates stable rotor operation throughout the flow range tested. The rotor stall point although not precisely measured, was found to occur at a  $C_x/U$  of approximately .35, far below the stator stall point as designed. In contrast to the stator stall which was very "soft" and could only be detected by the hot wire,\* the rotor stall was accompanied by an audible change in the compressor operation and a substantial vibration of the unit.

The point of stall inception was determined from observations of a hot wire anemometer probe located approximately 1 blade chord downstream of the stator trailing edge at an immersion of 75%. The wire axis was oriented perpendicular to the axial and radial dimensions. Stall

---

\*The occurrence of this type of behavior had, in fact, been previously pointed out by Smith(12).



inception was not sudden, that is a fully developed instability did not set in as the stall flow was reached. Instead the stall first appeared as a transitory phenomenon which gradually became fully developed as the compressor was throttled. Oscillograph traces\* of the developing stall for the treated and untreated cases are shown in Figs. 10 and 11. Here the hot wire output for 3 flow coefficients is shown. The first trace shows the compressor in stable operation, the next shows the first inception of the stall instability, and the last trace shows the fully developed stall which appears after a 2% reduction in flow from the point of first inception. Comparison of the inception and fully developed stall traces shows that the hot wire signal at inception lacks the regularity of the fully developed stall, which shows a repetitive pattern indicative of rotating stall. Comparing the first stall to the stable traces however shows that although irregular, a definite instability has set in. The flow coefficients corresponding to the inception traces then defines the stall points, which were determined to be .53 and .52 for the untreated and treated cases respectively.

In addition to determination of the stall points the hot wire is also useful in the isolation of the stall "source". Figures 12 and 13 are examples of the stall signal downstream of the stator at five radial location for the treated

---

\* These traces were retraced by hand to enhance their clarity

and untreated cases. Both figures show a very flat signal at the 10% immersion position and only a slight indication of an instability at 25%. At 50% immersion however the stall is quite evident and increases in amplitude as the hub is approached. It thus appears as if the compressor is hub limited as desired, although the stall is not confined to the hub endwall boundary layer region. In Figs. 14 and 15, stall signals at 75% immersion taken just ahead of and just behind the stator are given for the two configurations. Here the largest amplitudes are seen behind the stator which indicates stall originating in the stator passage. Thus, from this data, it appears as if the design objective of the stator hub being stall limiting has been met, and as will be discussed below it is likely that a blade stall is occurring.

Plots of the frequency spectrum for the untreated compressor in stable operation and stall are shown in Figs. 16 and 17. Here the stall appears not as a discrete "spike", but as a hump of considerable bandwidth. This is probably due to the manner in which the data was taken and reduced. The FFT program used a ten second record of digitized data to calculate the spectral components and since the stall frequency is not very steady, we expect to see the stall signal distributed over a wide frequency band. Comparison of the stall plot in Fig. 17 to the stable plot in Fig. 16 distinctly shows the evidence of the stall, with the so called "hump" completely absent in the stable case.

Although it is difficult to say with certainty with only one hot wire probe, that the stall is rotating, the frequency domain analysis tends to support this.

### 3.2 COMPRESSOR PERFORMANCE

#### A. Comparison to Design

In this section it is desired to compare the measured radial profiles of total pressure and flow angle to the original design prediction. In Fig. 18 the inlet total pressure traverse data taken at station 1 is compared to the design curve derived from Gopalakrishnan's data (Ref. 8). These profiles are very similar, the major difference being a somewhat thinner casing boundary layer exhibited by the present data. However, the general profile shape, which shows slightly higher losses at the O.D. is preserved. As previously discussed in section 2.5, this profile was integrated to obtain the mass flow rate.

A comparison of the inlet guide vane turning to design is presented in Fig. 19. Here the two profiles are nearly identical. Both curves indicate some overturning near the casing endwall, which is evidently associated with a secondary flow in this area.

Figure 20 compares the rotor total pressure profile at the stall point to the design prediction. It is recalled that the design philosophy is to have substantially lower total pressure rise across the rotor hub, and consequent low axial velocity and static pressure, and high flow angle at the rotor hub discharge to facilitate a stator hub stall. In this context the actual performance is even "better" than expected since the data shows a somewhat higher radial  $P_T$  gradient than predicted. In Fig. 21 the absolute air angle behind the rotor is compared to prediction. Here the profiles compare very well except near the casing

endwall. It is not known for certain what the source of this discrepancy is, but it may be due to a change in the local endwall flow blockage from that implied by the Gopalakrishnan data, a result of the casing treatment. It is noted here that the design program did not have the capability of radial adjustment of the blockage.

Completing the comparison to design, Fig. 22 compares the untreated stator discharge air angles to Carter's rule. Since the stator is stalled it is not surprising to find a substantial increase in stator deviation over Carter's rule over much of the annulus. This high deviation is not confined to the endwall region as one might expect if a pure wall stall were present. On the contrary it appears as if most of the blade span is stalled. Only at the O.D. does experiment compare with Carter's rule, which would seem to indicate a comparatively low loading at the stator casing.

#### B. Comparison of Treated and Untreated Compressor Performance

In this section we will show the effects of stator hub treatment on the compressor at the stall point. Presented in Figs. 23 and 24 are radial plots of the rotor and stator total pressure for the treated and untreated cases respectively. Since we would not expect the application of hub treatment to significantly affect the rotor performance, it is not surprising to note a strong similarity between the two rotor profiles. Of interest

here are the stator profiles, and in particular the change in total pressure across the stator. Here we note there are some subtle differences. The stator total pressure drop is essentially the same from the O.D. to  $R/R_T \sim .9$  (40% immersion), but below this radial location there is a larger total pressure drop for the untreated case, especially in the midspan region. As previously discussed, casing treatment studies have shown that a significant reduction in losses and flow blockage is a characteristic of treatment. While these effects are most evident near the endwall, improvement of the midspan region has been observed for some configurations (Refs. 1 and 3). However it is curious that the hub treatment data shows no apparent improvement in the hub endwall region but only in the 40% to 75% immersion area.

This improvement in the treated stator midspan is even more evident in a comparison of the treated/untreated stator exit air angles as shown in Fig. 25. As with the total pressure data, no improvement of stator turning is seen at the hub, but a substantial increase in turning ( $5^\circ$ ) due to treatment is seen in the midspan. It is noted here that the increase in treated stator static pressure rise discussed in section 3.1 (Figs. 7 and 8) may be due to the midspan improvement. This subject and its possible implications are discussed further in section 3.3.

## C) Comparison of Treated/Untreated Stator Wake .

## Traverses

In this section we will examine the circumferential traverses of the stator wakes, for the treated and untreated configurations at the stall point, in an attempt to understand the nature of the stall in both cases. Since the question of wall stall vs. blade stall appears to be of importance in the understanding of treatment effects (see Ref. 1), we will first seek to characterize the stall in this regard.

Presented in Figs. 26 and 27 are circumferential plots of the stator total pressure loss and deviation angle respectively, at the pitch diameter, for the untreated stall point and maximum flow point. If a blade stall is present at this radius, we expect a substantial increase in the wake thickness as we proceed from a stable to a stalled flow regime. This is quite evident in Fig. 26 with the profile at  $\phi = .62$  showing a sharp and narrow wake and a substantially thicker wake for the stalled case. The deviation angle plots in Fig. 27 also show this increase in wake thickness. It would thus appear as if a pure wall stall is not present for this configuration, which is seen as a key reason why the treatment was ineffective in stall margin improvement.

Analysis of stator wakes at several immersions is useful in addressing the question of a limiting stator hub. Circumferential traverses at 10%, 50%, 75% and 90% immersion for treated and untreated stator are shown in Figs. 28 through

31. In Figs. 28 and 29 the total pressure loss is shown. Here both the treated and untreated data show a fairly narrow wake near the casing but a substantially thicker wake at immersions of 50% and greater. In addition the level of total pressure loss increases as we approach the hub end-wall. Thus it appears as though the stator loading is indeed biased to the hub as desired. The treated/untreated deviation wake profiles in Figs. 30 and 31 exhibit similar radial characteristics.

Comparison of Figs. 28 and 29, and Figs. 30 and 31 also shows some interesting features of the treatment effects. The total pressure wake profiles in Figs. 28 and 29 do not show any substantial changes in wake shapes due to treatment except at 50% immersion. Here the wake is somewhat thinner and has a slightly lower loss level with treatment. The large increase in stator turning in the midspan due to treatment discussed above is also seen in a comparison of the deviation wakes at 50% and 75% immersion in Figs. 30 and 31. Here we note that the deviation levels are considerably ( $5^\circ$ ) higher for the untreated case, and that the treated wakes are slightly thinner and have lower amplitudes. This is particularly evident at 75% immersion. This change in wake shape is also seen at 90% immersion but is very small. Note here that the level of deviation at this location is actually higher ( $4^\circ$ ) in the treated data. In this region the slope of deviation angle vs. radial distance is very large however, and the observed increase could be caused by



a small shift in the hub streamlines due to the treatment. The wedge probe could also be seeing an increased tangential velocity component in the hub endwall region due to the treatment, with the endwall flow being "dragged" by the hub, as suggested in Ref. 11.

### 3.3 ANALYSIS USING THE AXISYMMETRIC DESIGN PROGRAM

In this section the axisymmetric compressor design program previously described in section 2.1 is used to determine the radial profiles of D-factor,  $\Delta P/q$ ,  $C_x$ , and  $\bar{\omega}$  at stall, as implied by the treated and untreated data. In this analysis the flow is first set to match the inlet wall static pressures as measured at the stall point. Streamline values of relative air angle ( $\beta_2$ ) and relative total pressure loss coefficient ( $\bar{\omega}$ ) are then iterated until a satisfactory match of the rotor total pressure and absolute air angle profiles is obtained. The measured stator discharge air angle profiles are directly input, and the  $\bar{\omega}$  profiles iterated until the stator total pressure data is matched. At each iteration, station blockage factors are adjusted to match the interstage wall static pressures. It is noted here that since the radial traverse data used in this analysis was taken in the 5% to 90% immersion range, any results shown that are outside this range represent an extrapolation.

Figures 32 and 33 show a comparison of the untreated rotor/stator D-factor and  $\Delta P/q$  profiles derived from this analysis. The D-factor profiles in Fig. 32 show a fairly

flat rotor load profile, with the normal increase at the endwalls. This profile is typical of a lightly loaded rotor operating near the design point, with no portion of the blade having an excessively high aerodynamic loading. The stator D-factor profile, however, is highly biased at the hub and exceeds the "stall criterion" of .6 at about 75% immersion. This criterion is thus conservative for this compressor. Comparison of the D-factor profiles to the design curves shows a higher level of D-factor for both rotor and stator and a somewhat smaller rotor/stator load split for the test data. The higher load level at stall is due to the conservative stall criterion used for the design case, and the relatively higher rotor load due to an underestimate of the stator deviation in the design. Comparison of the stator D-factor profile to design also shows a higher hub bias for the test data, which was indicated previously in a comparison of the rotor total pressure profile to design (see Fig. 19). The stator  $\Delta P/q$  profile shown in Fig. 33 also shows the high hub bias, but the level is substantially below the D-factor, thus indicating the possibility of a blade stall. The rotor  $\Delta P/q$ , as well, is sufficiently low as to exclude any apparent aerodynamic difficulty. Thus from this comparison it appears as if the design objective of a substantial rotor/stator load split, and a high stator hub load bias has been met.

Figure 34 compares the treated and untreated stator D-factor profiles. Here the highest levels at the hub are the same for both cases. At the midspan however, we do see

a higher level for the treated case, evidently a result of the higher static pressure rise and turning observed in this area. The increased static pressure rise of the treated stator is also seen in the plot of  $\Delta P/q$  profiles in Fig. 35. Here the increase in  $\Delta P/q$  level is essentially constant at all radii.

The effect of the treatment on the radial distribution of axial velocity can be seen in Fig. 36. As we might expect from some of the previous comparisons, the treatment results in an increase in axial velocity in the midspan and a slight reduction at the endwalls. Figure 37 shows the effect of treatment on the implied  $\bar{\omega}$  profiles. Here again the treatment has apparently improved the flow in the midspan. The computer analysis is thus consistent with the experimental results which indicate that the application of stator hub treatment to the geometry tested in this experiment results in a reduction of flow blockage not at the hub endwall, but in the midspan of the blade row.

### 3.4 DIAGNOSTIC TESTS

In addition to the data presented in the foregoing sections, other data of a diagnostic nature was also taken to investigate the sensitivity of the results to the particular experimental conditions that were examined. These tests are briefly reported below.

#### A. Reynolds Number Effects

It has been shown that the stall margin of an axial

flow compressor may be subject to substantial variation if the Reynolds number based on blade chord falls below a critical value. In Ref. 13, C. Lakhwani and H. Marsh reported a "critical" Reynolds number of approximately  $1.0 \times 10^5$  for a rotor in a single stage. Below this, the axial velocity parameter at the stall point was observed to increase rapidly, while above this value there was little change. Greitzer also observed no significant change in stall point down to a Reynolds number of  $1 \times 10^5$  in experiments with a three stage compressor (Ref. 14). The experiments reported herein were at a Reynolds number of  $1.5 \times 10^5$ . However to ensure that Reynolds number effects were not significant the stall onset was investigated up to 3500 RPM, or up to a Reynolds number of approximately  $2 \times 10^5$ . These tests showed that the stall onset point was essentially constant over this speed range, thus assuring that Reynolds number effects were not significant in the experimental results.

#### B. Effect of Rotating Stall on Compressor Performance

Since the comparisons of the compressor performance with and without hub treatment discussed above were made at the stall point in the presence of some amount of rotating stall, it was necessary to ensure that the stall did not significantly affect the compressor performance and hence the comparisons. In particular it was desired to ensure that the stator performance (losses and turning) and wake characteristics did not change significantly as one progressed from a "near stall" point to the stall point. To investigate

this possibility, a circumferential traverse of the untreated stator exit at the pitch diameter was taken at a flow coefficient of .55, 5% above the point of stall inception. At this flow point, the hot wire signal at stator exit showed no evidence of stall instability. This traverse showed a slightly lower total pressure defect in the wake compared to the stall point traverse, but the wake shape and deviation level had not changed appreciably. A radial traverse of the stator exit at this flow point showed virtually no change from the stall point data as shown in Fig. 38, thus indicating that the inception of rotating stall did not result in a step change in the stator performance.

## CHAPTER 4

## CONCLUSIONS AND RECOMMENDATIONS

## 4.1 SUMMARY AND CONCLUSIONS

The application of axial skewed slots to the rotating hub under a compressor stator did not result in a significant change in the stall onset point of the stator. Although a hot wire survey of the flow showed that the stator hub region was indeed (stall) limiting, the stall was not confined to the endwall and was observed out to the midspan. Circumferential traverses also indicated that the stator wakes were severe over a substantial fraction of the span. This points to the fact that the stator experienced a blade stall rather than a wall stall, and this is seen as a key possibility for the lack of stall margin improvement.

Although the effect of hub treatment on stall margin was small, the treatment did result in a significant change in the stator performance at the stall point. Most notably the stator deviation angles were substantially reduced by the hub treatment in the middle 30% of the annulus. This increase in turning was also seen in a comparison of the wake traverses in the midspan region. In addition to the improvement in turning there was an apparent reduction in total pressure loss across the stator midspan, as indicated by the analysis of the data with the axisymmetric design program. Analysis of the treated and untreated data using the axisymmetric design program also showed that the treatment had resulted in a slight increase in the axial velocity in the midspan and

confirmed the observation of a reduction in total pressure loss. Thus it seems clear that the flow blockage has definitely been reduced in the stator midspan.

The hub treatment was also observed to affect the stator wake shapes in the midspan region. In the configuration with the treated hub at the 50% and 75% immersion levels the wakes were thinner and had lower amplitudes than the wakes with the smooth hub. It is possible that the wake thinning and performance improvement in the midspan is due to the presence of a strong secondary flow induced by the treatment, similar to that noted by Mikolajczak and Pfeffer in Ref. 11. These flows are observed to "aspirate" the low energy fluid on the blade suction surface and should thus cause a thinning of the wake on the suction side. However, with the exception of the air angle wake traverses at 75% immersion, the wake thinning due to treatment was small, and the axial placement of the traverse probe (1.0 blade chord downstream of the stator trailing edge) made it very difficult to determine which side (pressure or suction) of the wake had been thinned. Thus, although supportive, the data is not conclusive in this regard.

In addition to the effects discussed above, the stator was observed to have a higher static pressure rise across it when run with the treated hub, than with the smooth one. This increase was seen at all flows tested, and is associated with the increase in turning, and reduction of losses, observed with the treatment. It would thus appear as if the treatment

effects are not confined to the stalled or near stalled flow regime, but are evident at all flow levels.

#### 4.2 RECOMMENDATIONS

Continued research in the subject of stator hub treatment should examine the question of its effect on stator stall with a wall stall configuration, as well as seek to determine the mechanism responsible for the midspan improvements. Concerning the question of stall margin improvement, an experiment should be conducted in which the stator hub endwall is the sole "source" of stall, i.e., no blade stall. As discussed above, the existence of a blade stall in this experiment is felt to be the key reason for the ineffectiveness of the treatment on stall margin. Thus, a clear wall stall experiment would be very informative as to the hub treatment stall effect. For the present compressor configuration we have pushed about as far as possible toward achieving this. However, with the installation of an exit fan, we will be no longer limited by the requirement of greater than ambient static pressure at exit and can thus consider configurations with a higher stator stagger in order to increase the  $\Delta P/q$  relative to D-factor. An increase in the solidity of the present blades would also be helpful in dropping D-factor, and blade stall might be inhibited by an increase in stator camber also. These effects should be examined and the compressor rebuilt in a configuration that is much more clearly in a wall stall situation. It should be emphasized that the criteria for wall stall vs. blade stall are still not certain and the obtaining of a definite wall stall is regarded as one of the more



uncertain features of the experiment.

As previously mentioned, the improvement in the stator midspan flow could be due to the action of a secondary flow induced by the treatment, in which low energy fluid in the stator suction surface boundary layer is entrained radially towards the hub. By taking stator wake traverses very close to the stator trailing edge, it may be conclusively determined if the treatment results in a thinning of the suction side of the midspan wakes, an expected consequence of the above hypothesis. Hot wire surveys of the stator passage and boundary layers could also serve to identify changes in the secondary flow characteristics due to treatment.

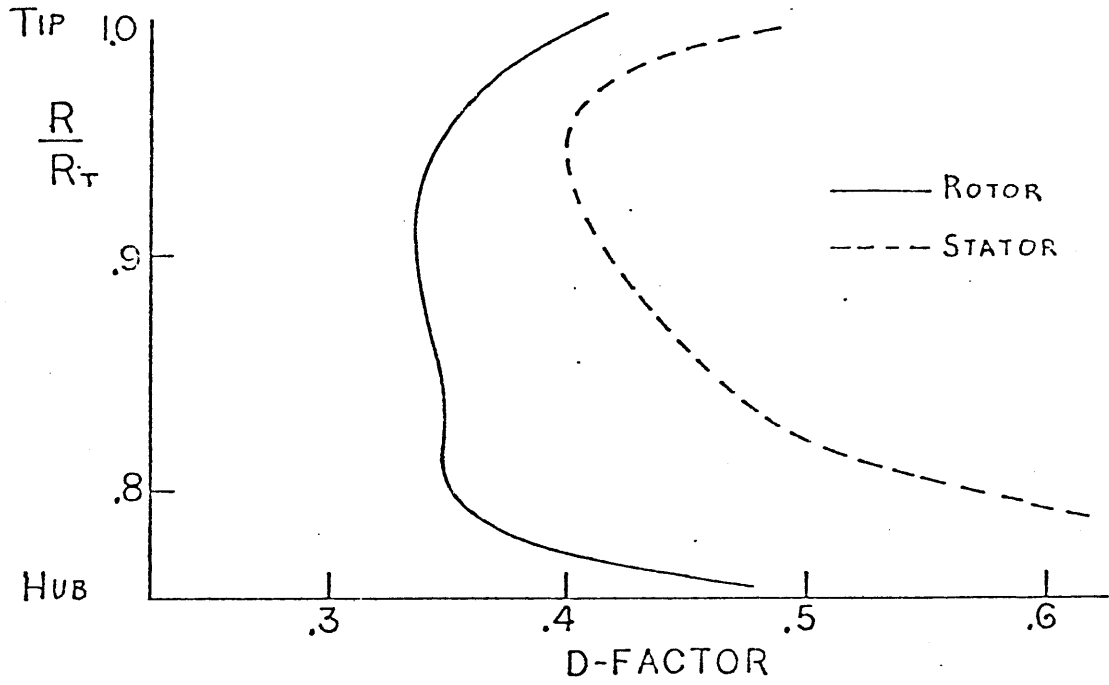
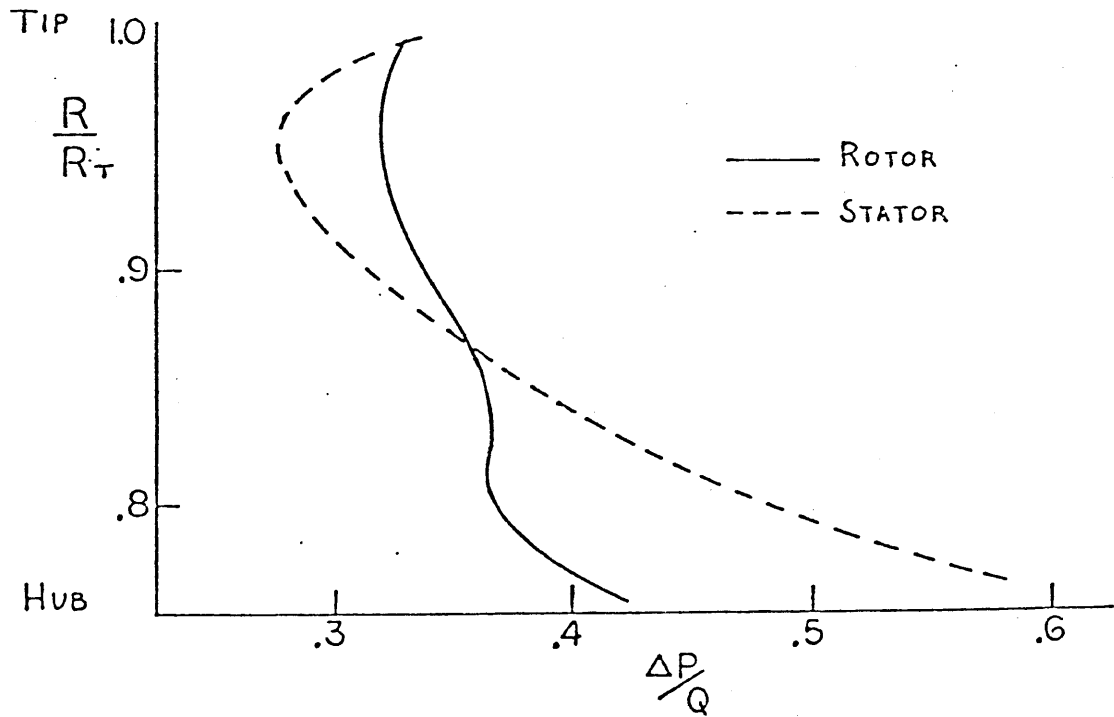
It would also be of interest to examine the slot flow itself and compare it to the well known observations of the casing treatment slot flows. This could best be accomplished via hot wire surveys of the stator endwall boundary layer region. Pressure and velocity traverses of the stator channel with a five hole probe as previously used by Smith (Ref. 2) could also contribute significantly to our understanding of the hub treatment effects.

## REFERENCES

1. Greitzer, E. M., Nikkanen, J. P., Haddad, D. E., Mazzawy, R. S., and Joslyn, H. D., "A Fundamental Criterion of Rotor Casing Treatment", ASME Journal of Fluids Engineering, June 1979, Vol. 101.
2. Smith, G. D. J., "Casing Treatment in Axial Compressors", Doctoral Thesis, Engineering Department, University of Cambridge, April 1980.
3. Prince, D. C., Jr., Wisler, D. C., and Hilvers, D. E., "Study of Casing Treatment Stall Margin Improvement Phenomena", NASA CR-134552, March 1974.
4. Takata, H., and Tsukuda, Y., "Stall Margin Improvement by Casing Treatment - Its Mechanism and Effectiveness", ASME Paper 76-GT-A, February 1976.
5. Wisler, D. C., Hilvers, D. E., "Stator Hub Treatment Study", NASA CR-134729, December 1974.
6. Jensen, W., Carter, A. F., Swarden, M. C., "Improvements in Surge Margin for Centrifugal Compressors", presented at AGARD 55th Specialists' Meeting, "Centrifugal Compressors, Flow Phenomena and Performance", Brussels, Belgium (1980).
7. Hearsey, R. M., "A Revised Computer Program for Axial Compressor Design", Vol. 1 and 2, ARL-TR-75-001, Aerospace Research Laboratory, Wright Patterson Air Force Base, Ohio, 1976.
8. Gopalakrishnan, S., "An Unconventional Blade Design for Axial Compressors", M.I.T., Gas Turbine Laboratory Report No. 98, May 1969.
9. Horlock, J. H., "Axial Flow Compressors, Fluid Mechanics and Thermodynamics", PP56-63.
10. Lieblien, S., "Experimental Flow in Two-Dimensional Cascades", Aerodynamic Design of Axial Flow Compressors, Chapter VI, NASA SP-36, 1975.
11. Mikolajczak, A. A., and Pfeffer, A. M. "Methods to Increase Engine Stability and Tolerance to Distortion", AGARD-LS-72, October 1974.

12. Smith, L. H., Personal Communication (1980).
13. Lakhwani, C., and Marsh, H., "Rotating Stall in an Isolated Rotor Row and a Single Stage Compressor", Conference publication 3, Institution of Mechanical Engineering, 1973.
14. Greitzer, E. M., "Surge and Rotating Stall in Axial Flow Compressors, Part II: Experimental Results and Comparisons with Theory", ASME Journal of Engineering for Power, Vol. 100, January 1978.

FIG. 1 D-FACTOR DESIGN PROFILES

FIG. 2  $\Delta P/Q$  DESIGN PROFILES

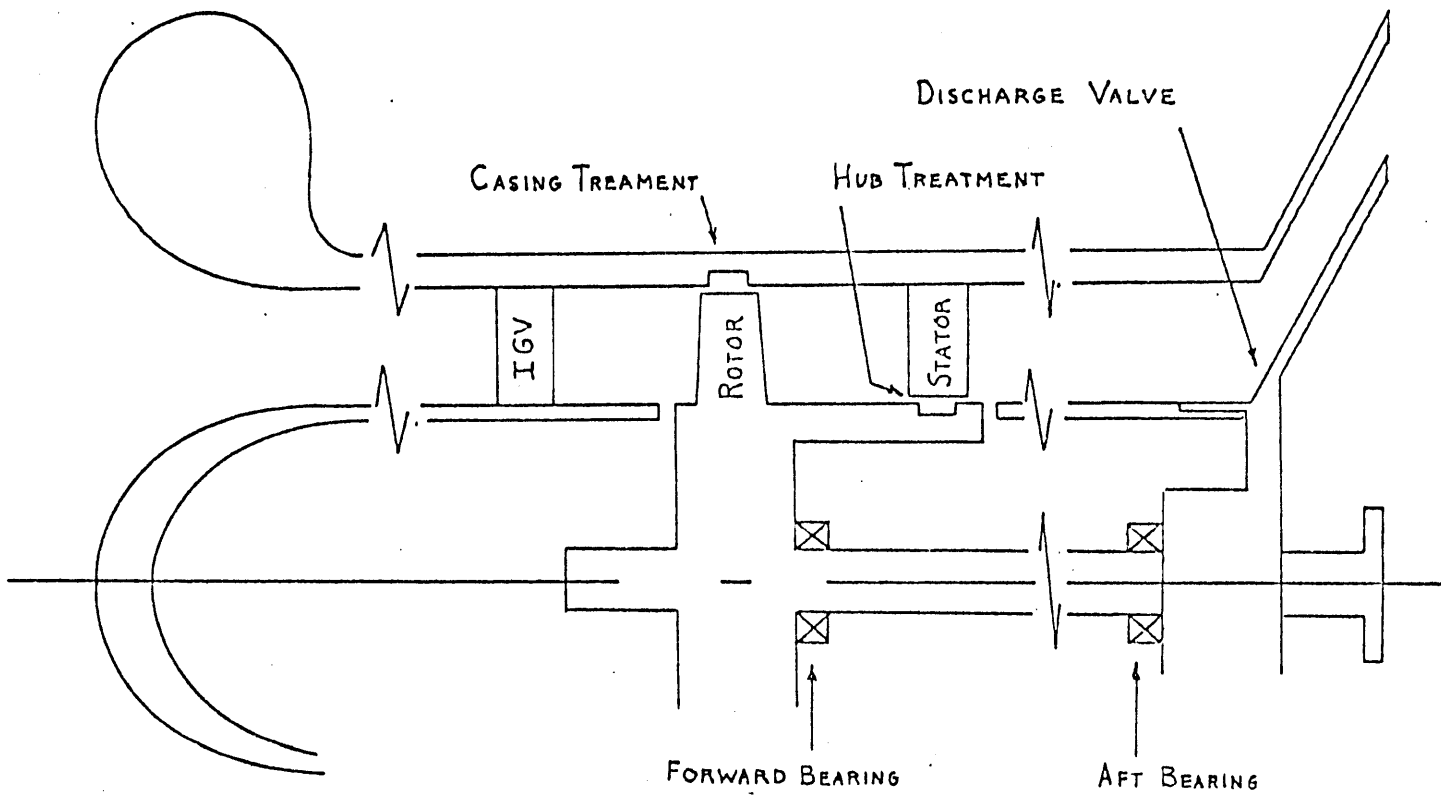
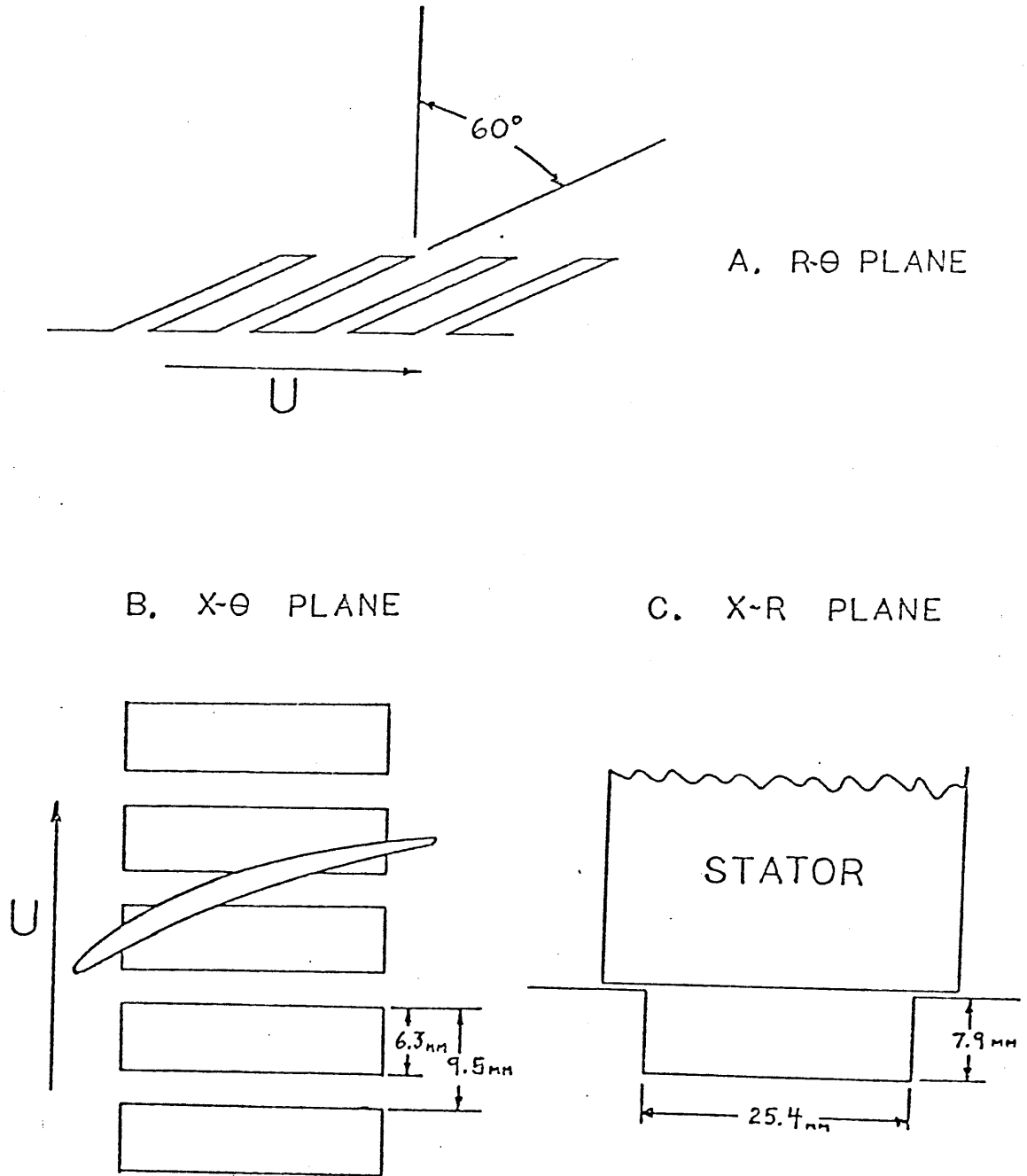


FIG. 3 COMPRESSOR CROSS SECTION

FIG. 4 HUB TREATMENT GEOMETRY



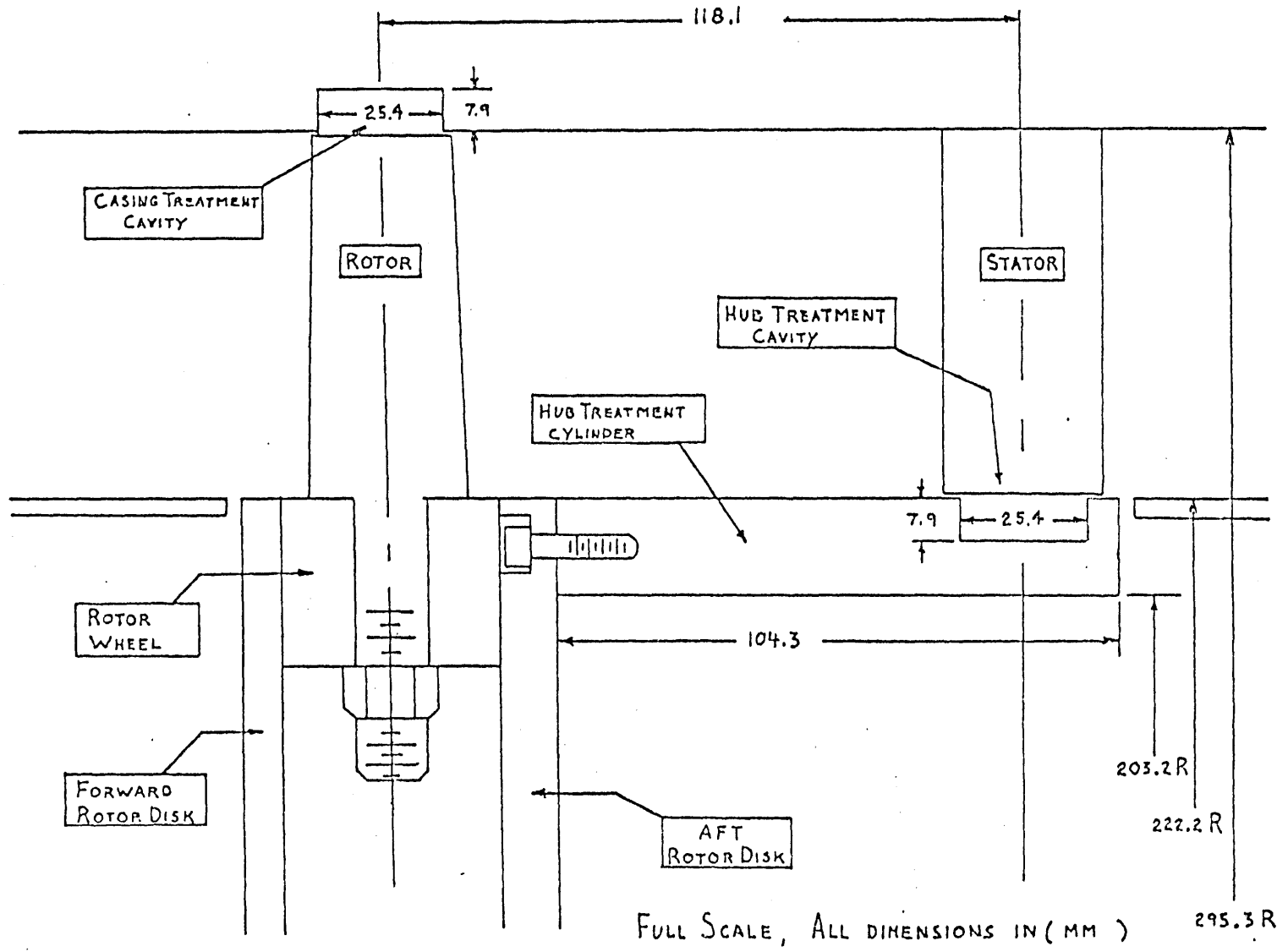


FIG. 5 ROTOR/HUB TREATMENT ASSEMBLY

FIG. 6 INSTRUMENTATION LAYOUT

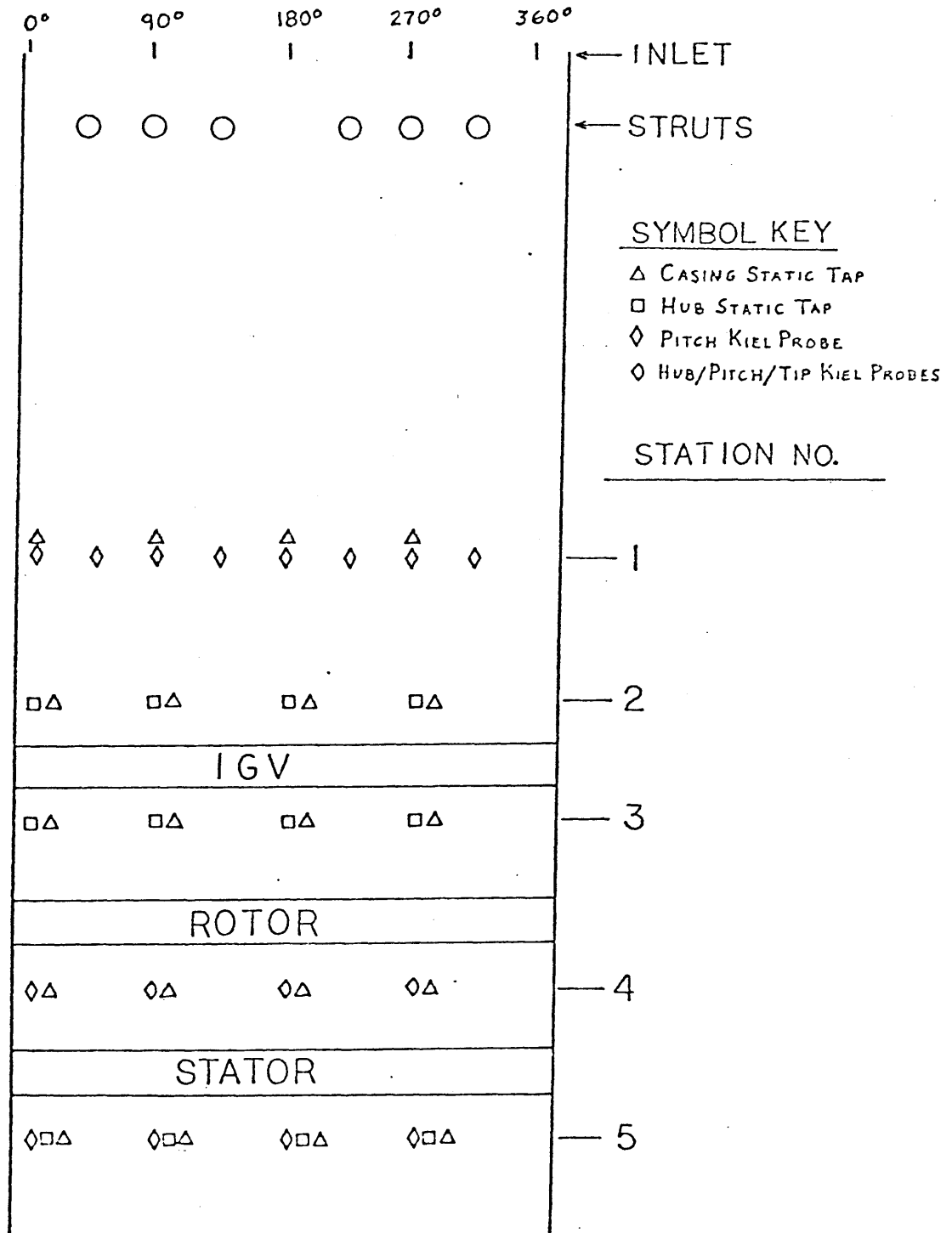




FIG. 7 OVERALL TOTAL TO STATIC PRESSURE RISE CHARACTERISTIC

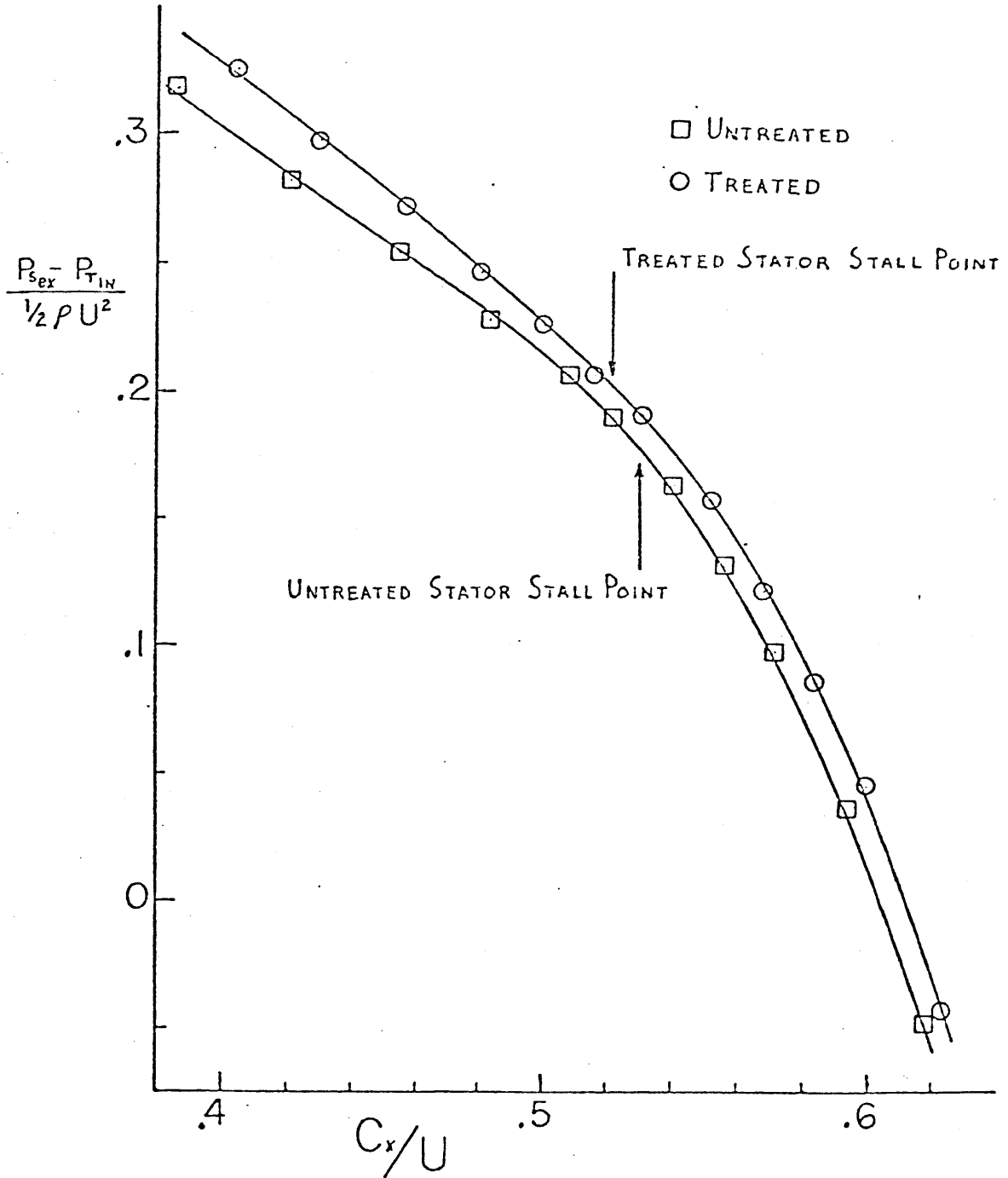


FIG. 8 STATOR STATIC PRESSURE RISE CHARACTERISTIC

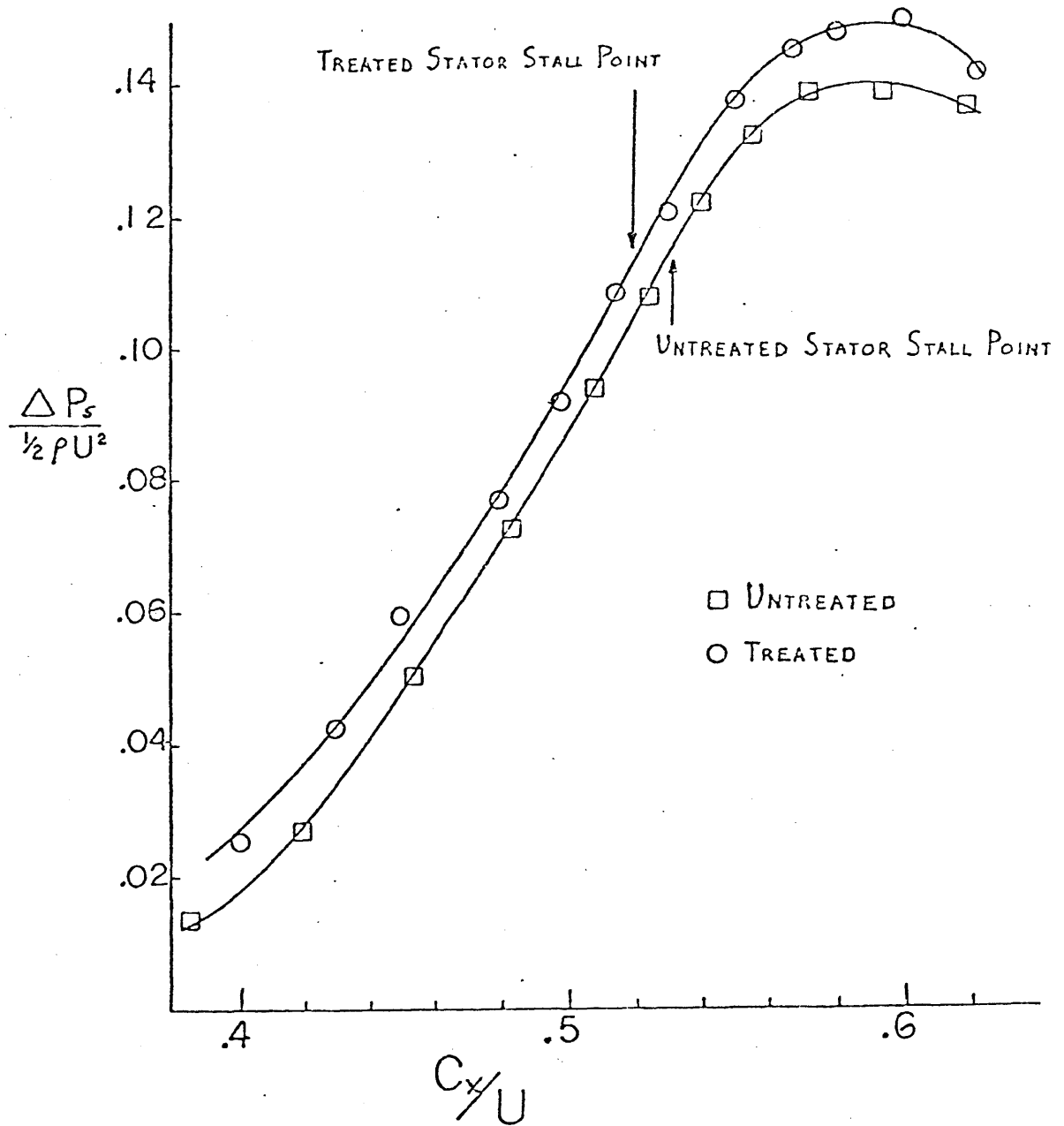


FIG. 9 ROTOR TOTAL PRESSURE RISE CHARACTERISTIC

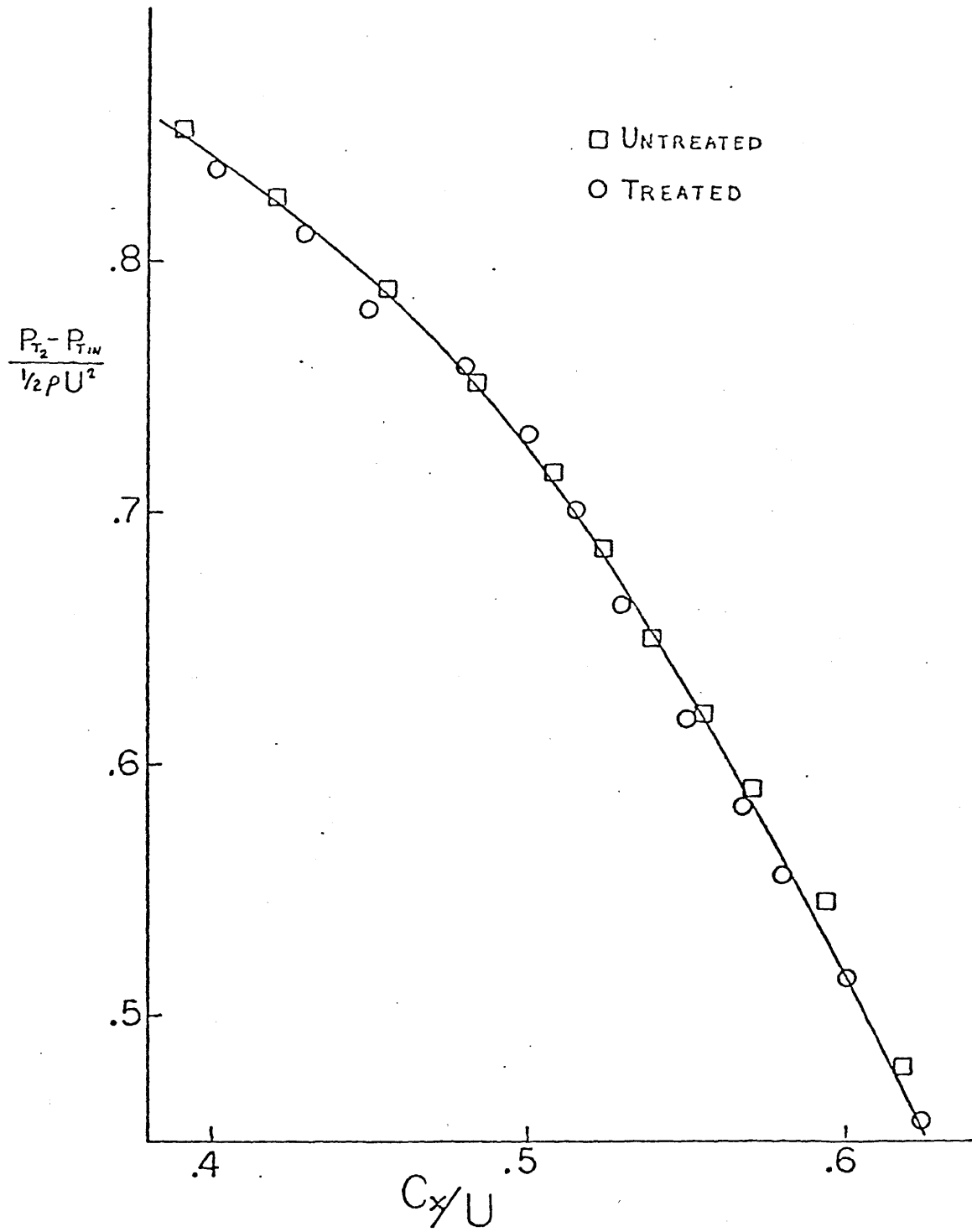


FIG. 10 HOT WIRE SIGNAL AT TREATED STATOR DISCHARGE,  $I_M = .75$ 

RELATIVE SCALE

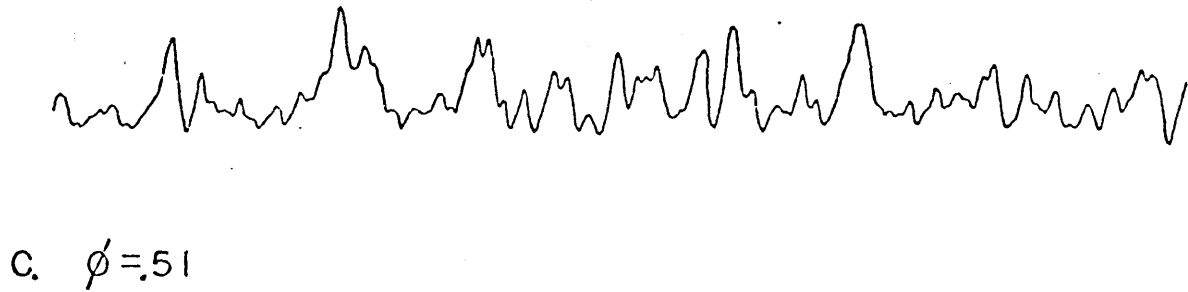
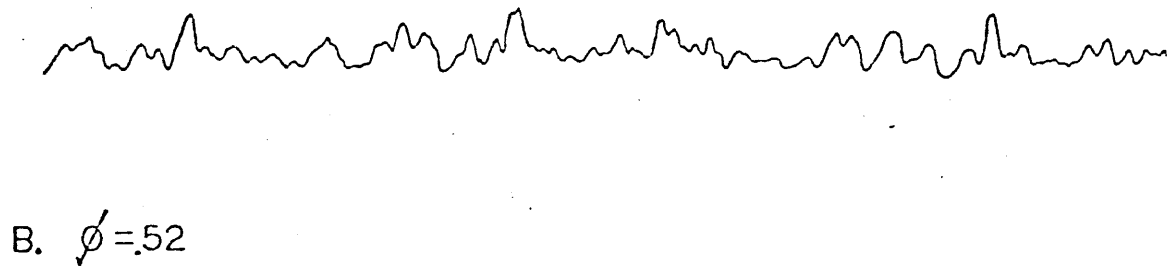
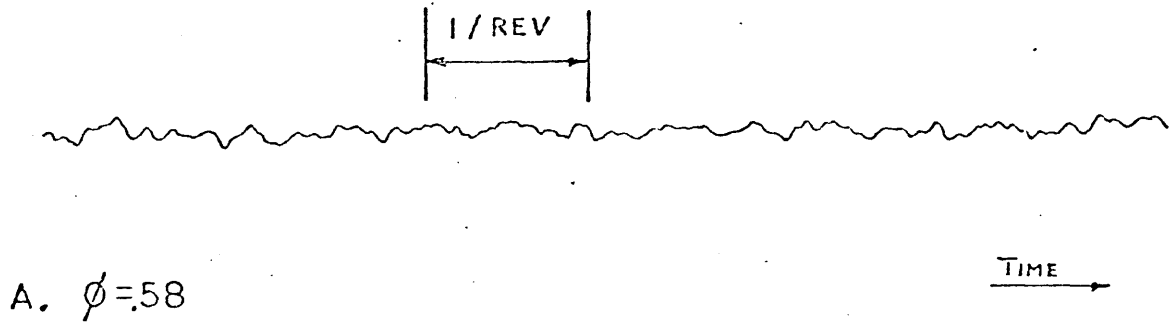


FIG. 11 HOT WIRE SIGNAL AT UNTREATED STATOR DISCHARGE,  $IM = .75$ 

RELATIVE SCALE

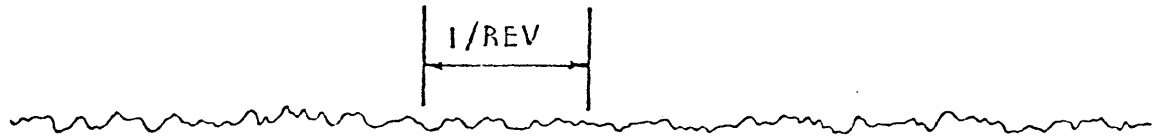
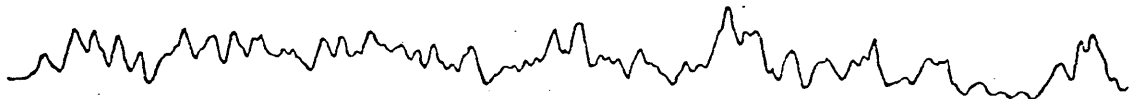
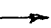
A.  $\phi = .58$ TIME B.  $\phi = .53$ C.  $\phi = .52$

FIG. 12 HOT WIRE SIGNAL AT TREATED STATOR DISCHARGE, STALL POINT

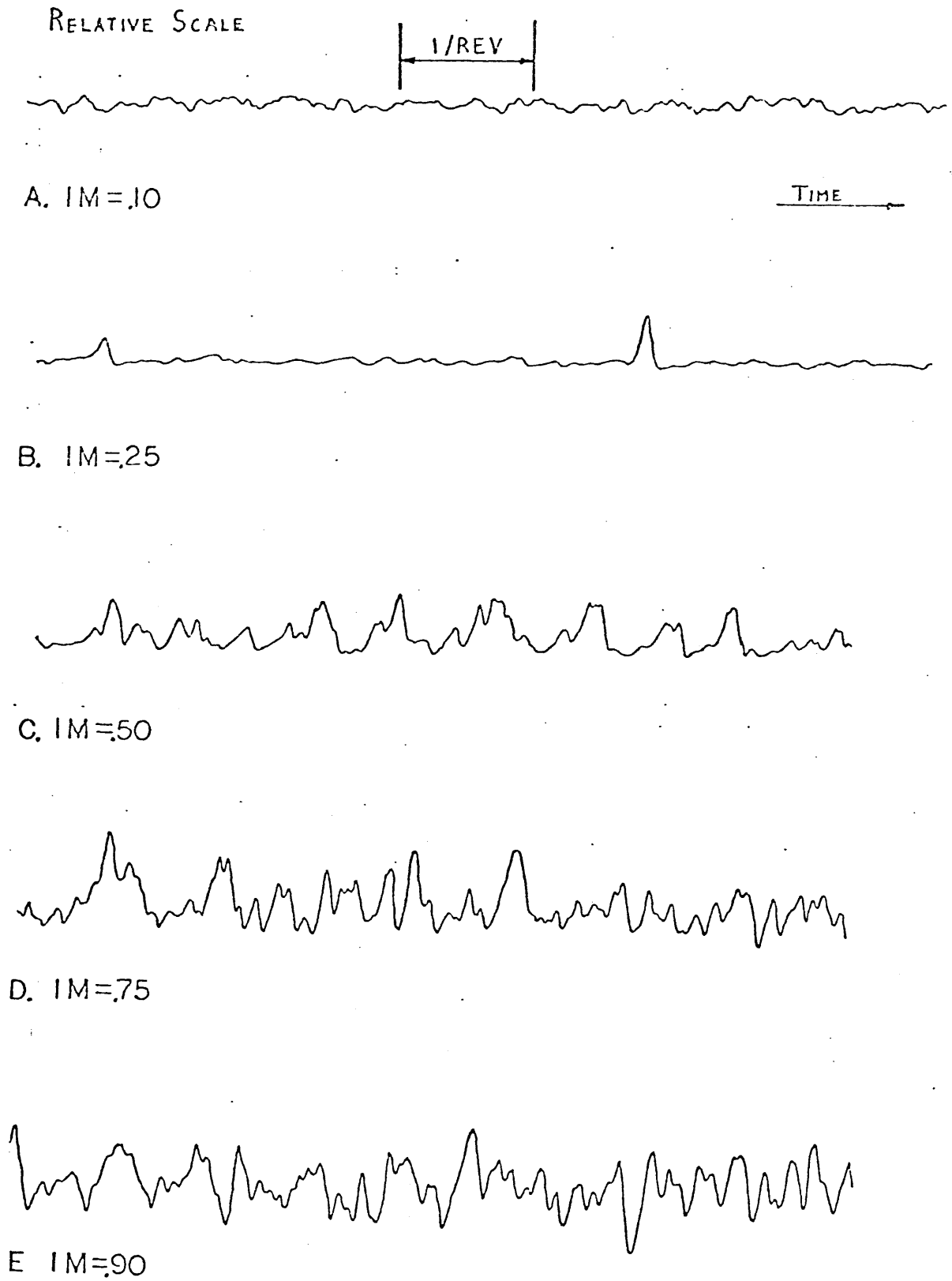


FIG. 13 HOT WIRE SIGNAL AT UNTREATED STATOR DISCHARGE, STALL POINT

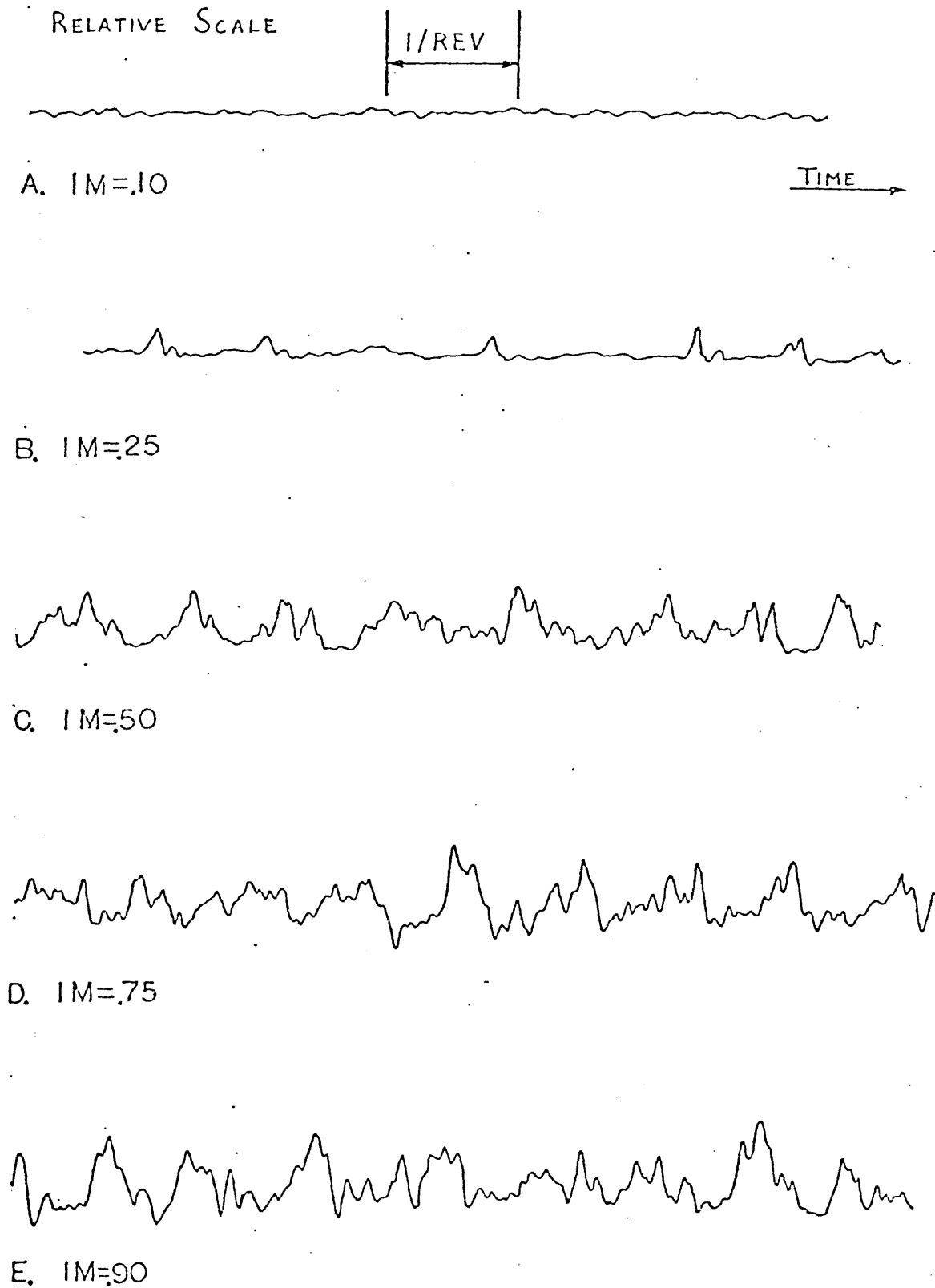


FIG. 14 HOT WIRE SIGNAL AT TREATED STATOR INLET AND DISCHARGE  
 $IM = .75$ , STALL POINT

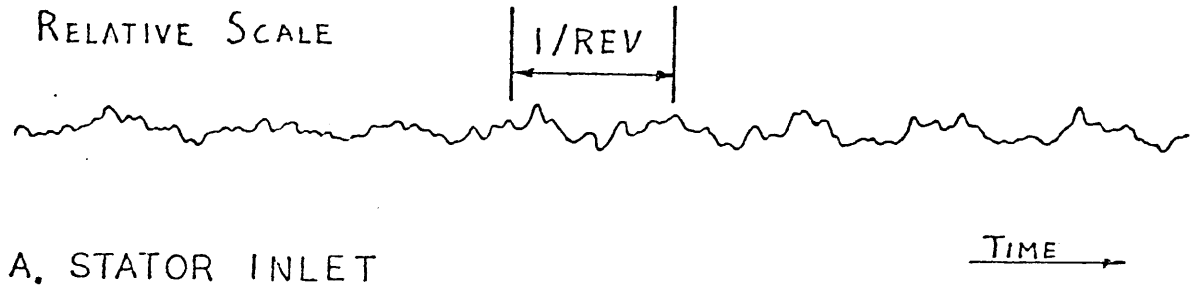


FIG. 15 HOT WIRE SIGNAL AT UNTREATED STATOR INLET AND DISCHARGE  
 $IM = .75$ , STALL POINT

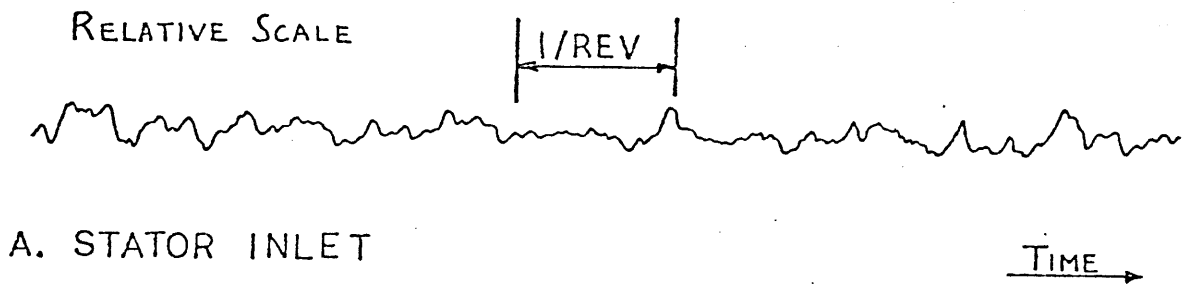
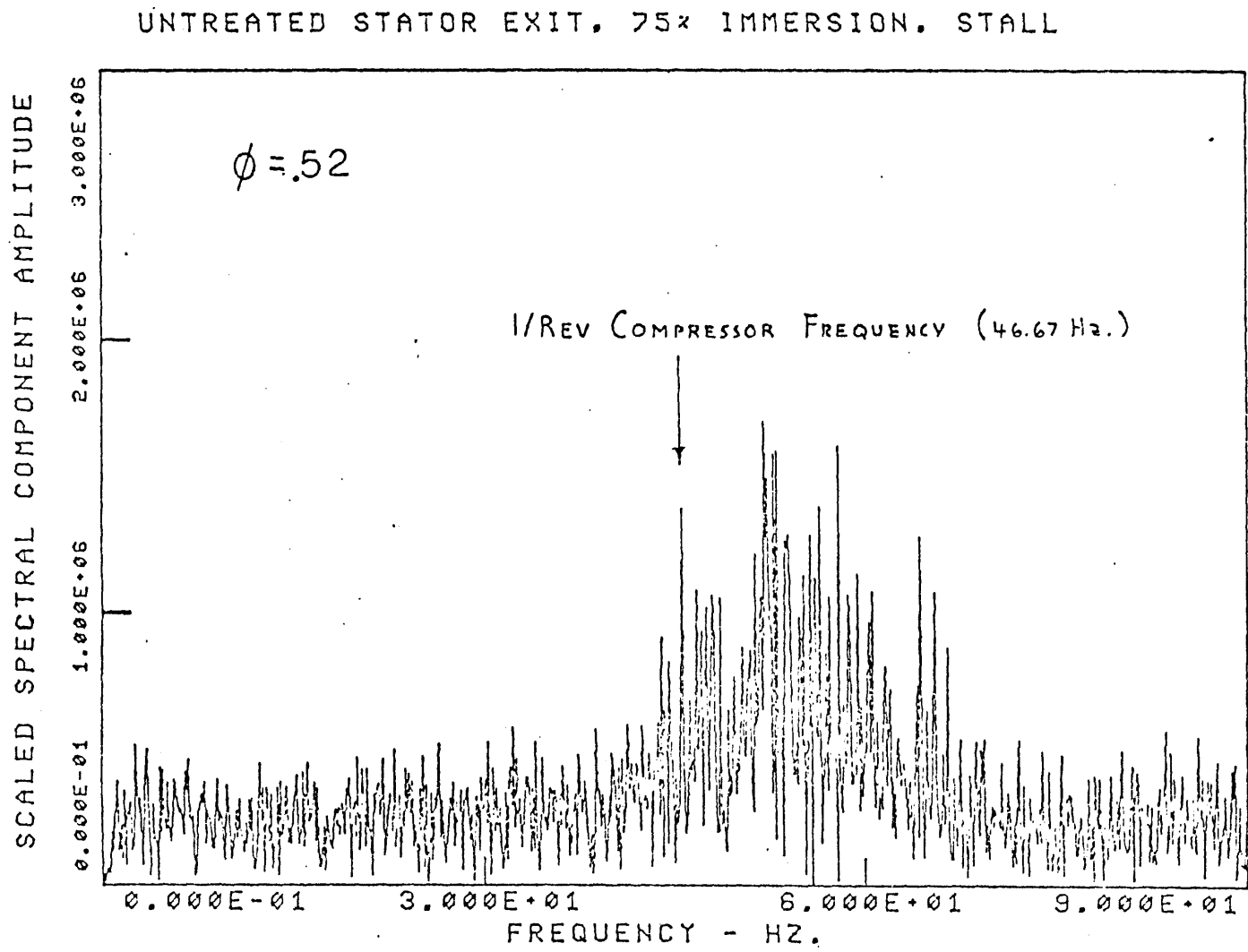




FIG. 16 F F T SPECTRUM OF STATOR HUB EXIT, STALL



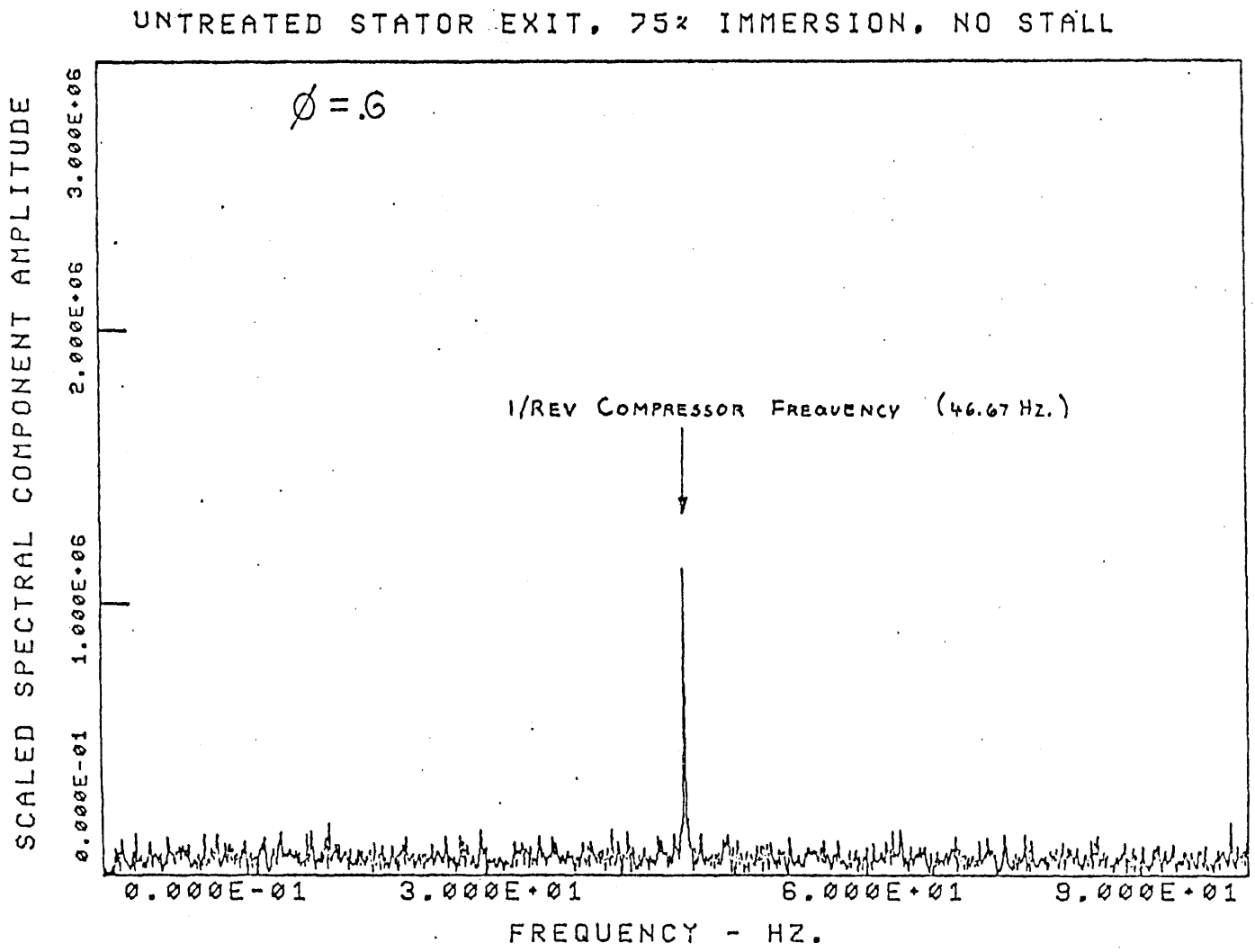


FIG. 17 FFT SPECTRUM OF STATOR HUB EXIT, NO STALL

FIG. 18 INLET TOTAL PRESSURE PROFILE VS. DESIGN

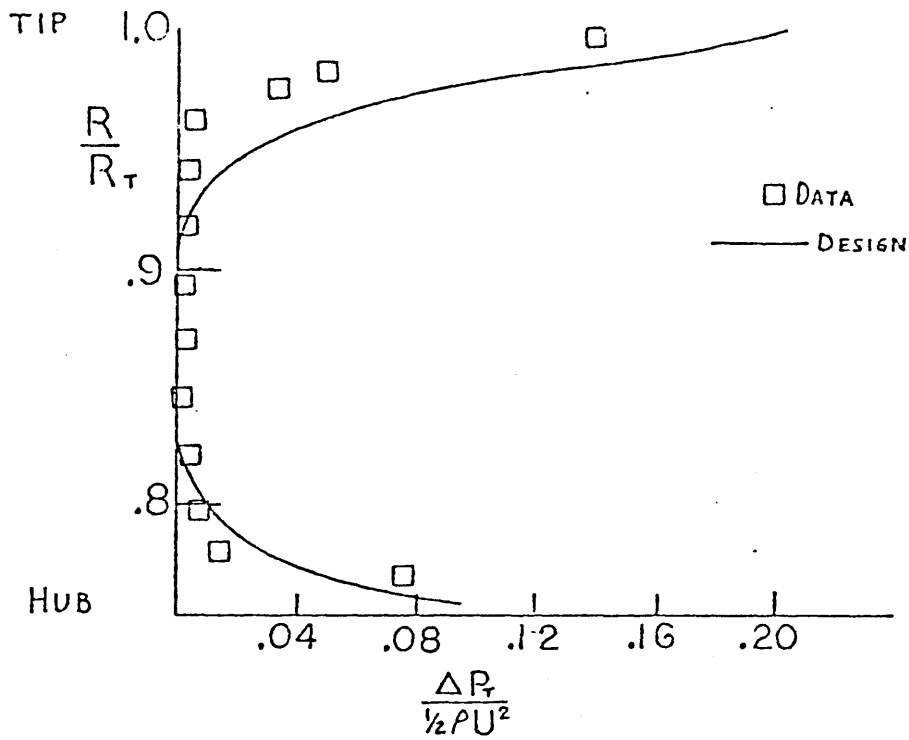


FIG. 19 IGV EXIT AIR ANGLE PROFILE VS. DESIGN

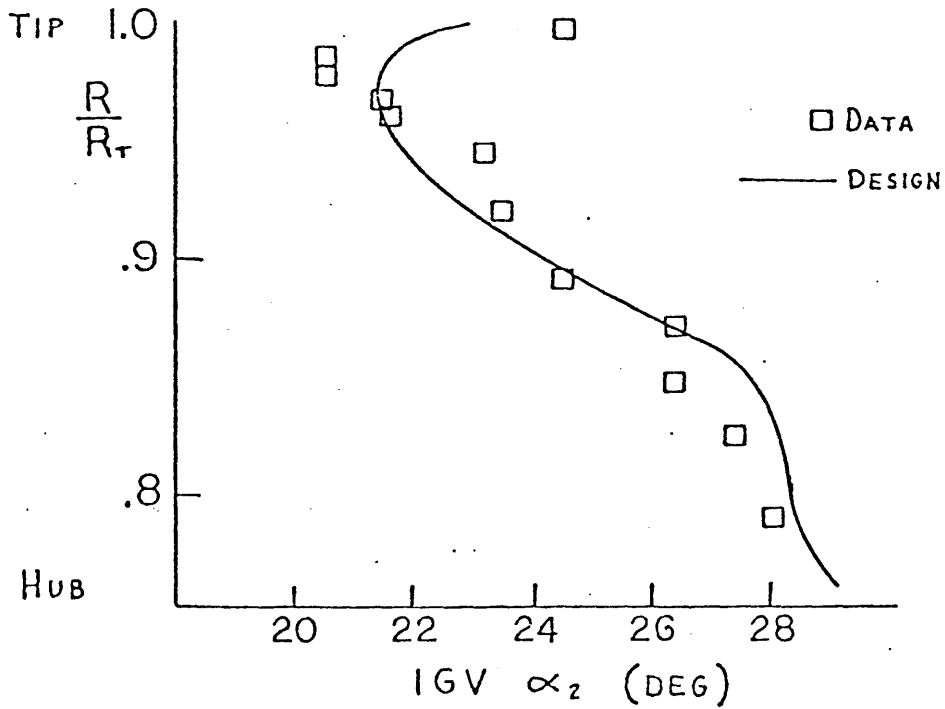


FIG. 20 ROTOR EXIT TOTAL PRESSURE PROFILE VS. DESIGN, STALL POINT  
TIP 1.0

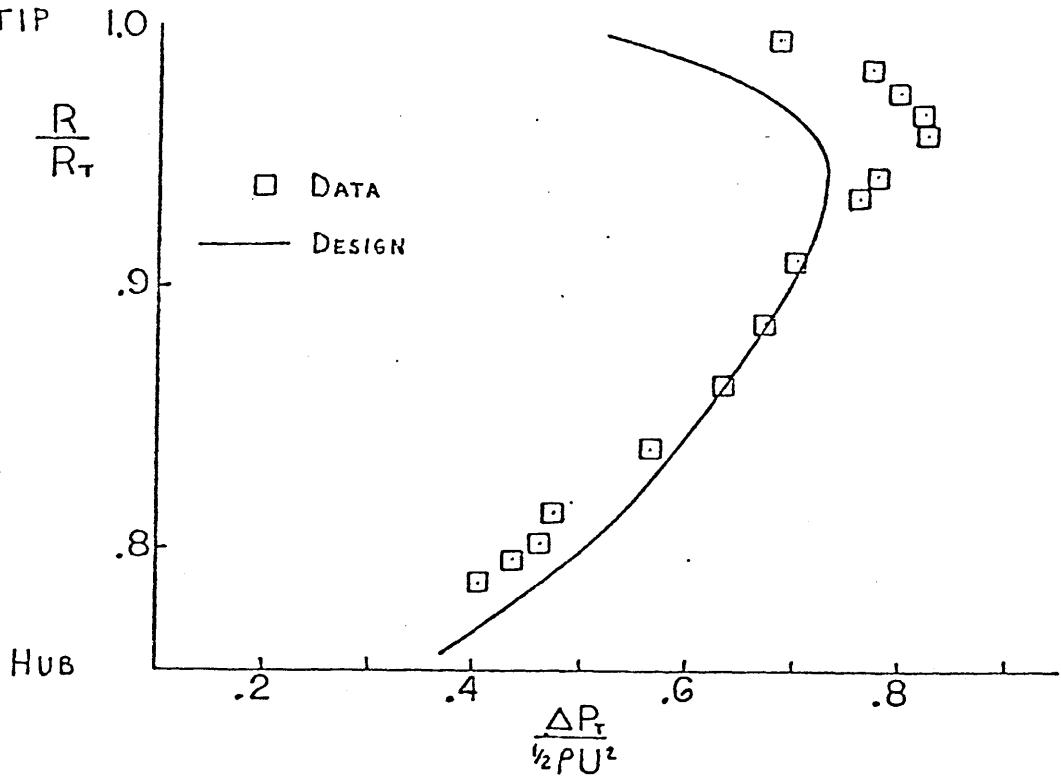


FIG. 21 ROTOR EXIT AIR ANGLE PROFILE VS. DESIGN, STALL POINT  
TIP 1.0

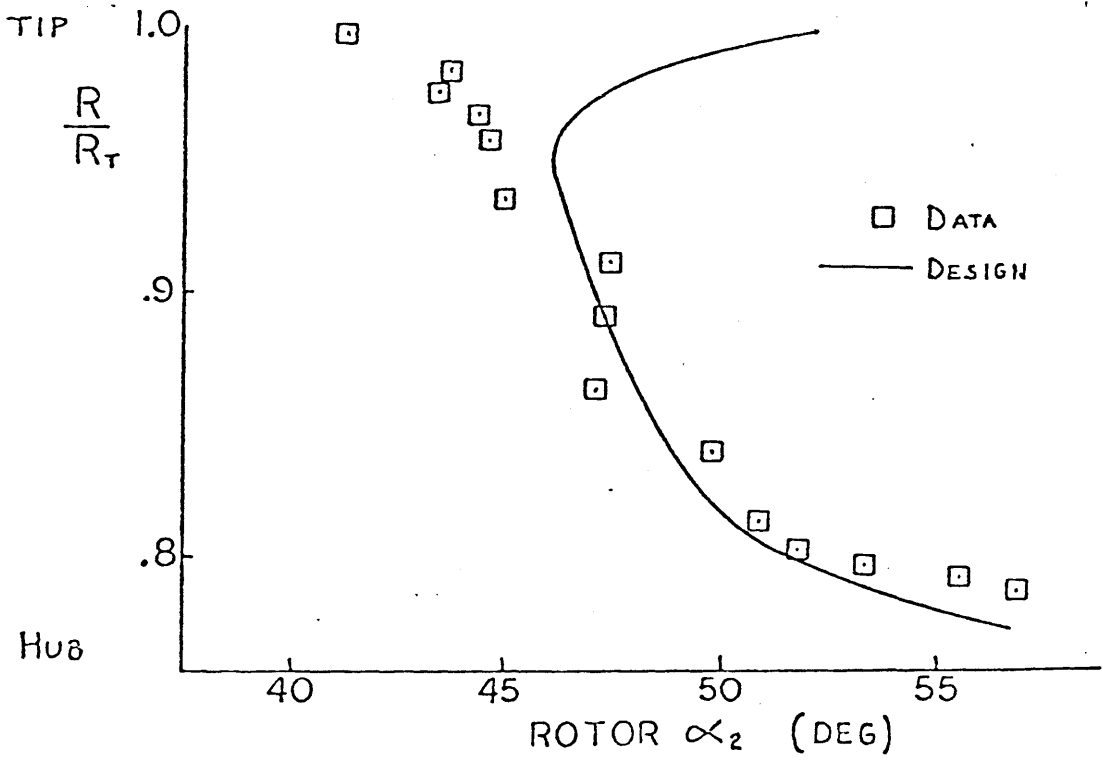


FIG. 22 UNTREATED STATOR EXIT AIR ANGLE PROFILE VS. CARTER'S RULE, STALL POINT

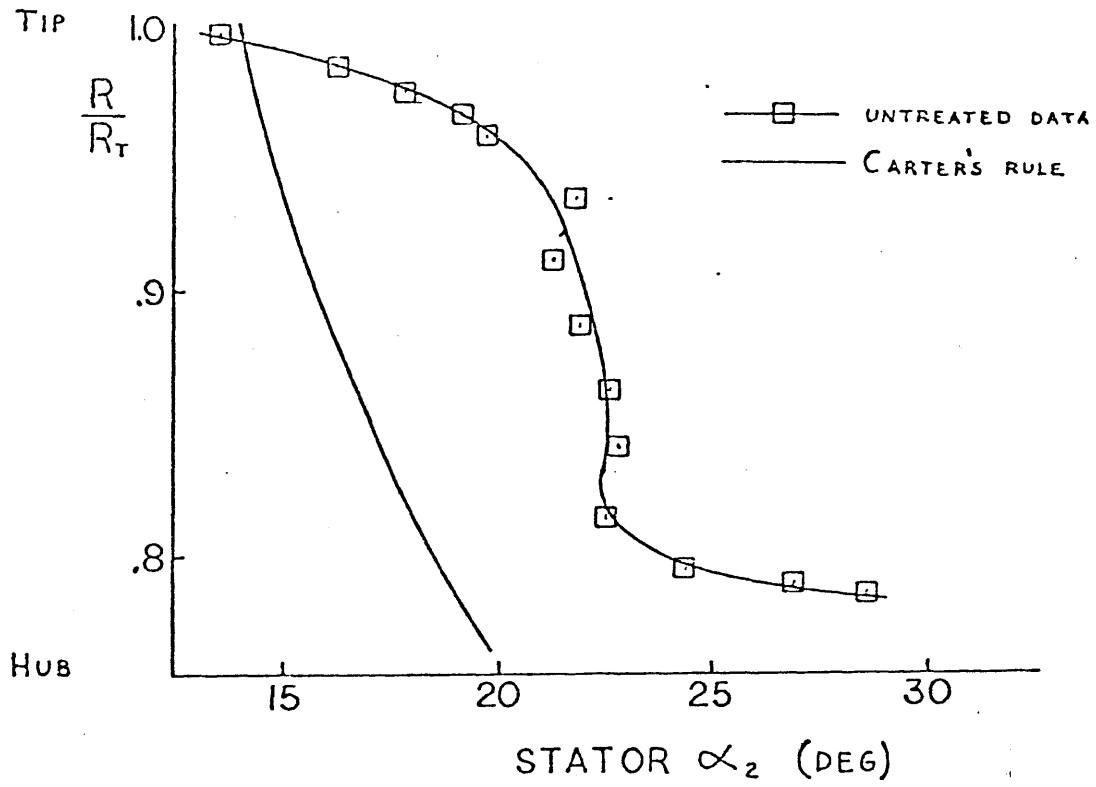


FIG. 23 TREATED HUB: ROTOR AND STATOR TOTAL PRESSURE PROFILE, STALL POINT

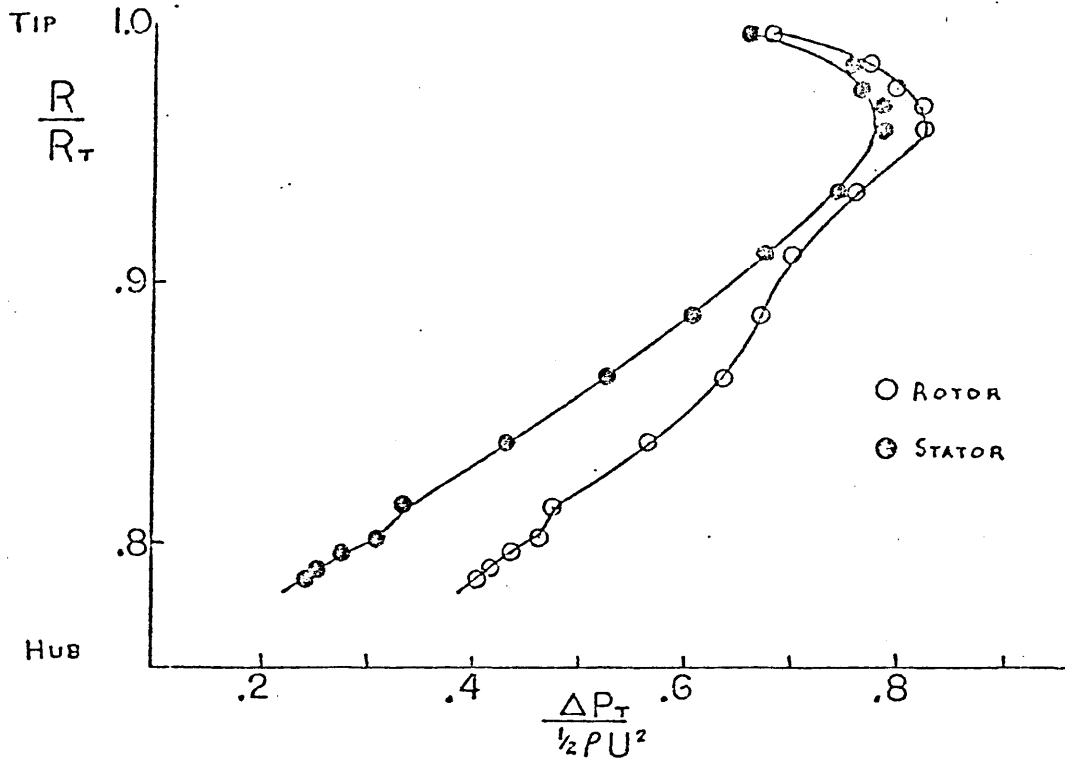


FIG. 24 UNTREATED HUB: ROTOR AND STATOR TOTAL PRESSURE PROFILE, STALL POINT

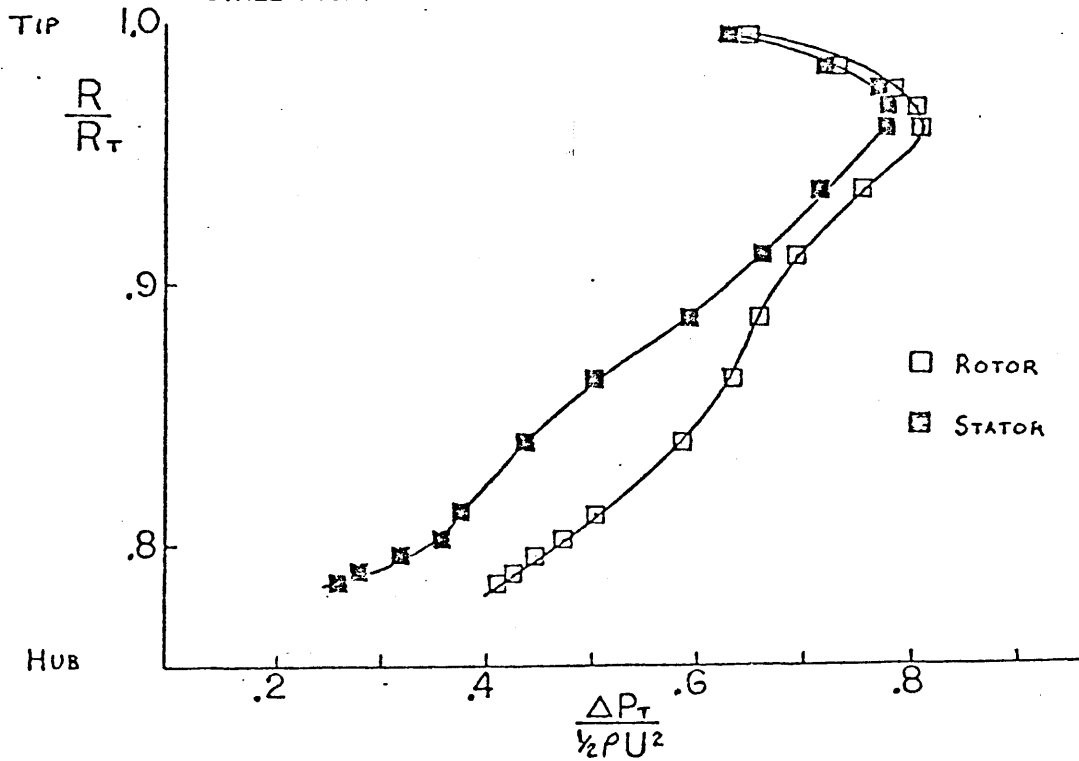


FIG. 25 STATOR EXIT AIR ANGLE PROFILE AT STALL POINT, TREATED VS. UNTREATED

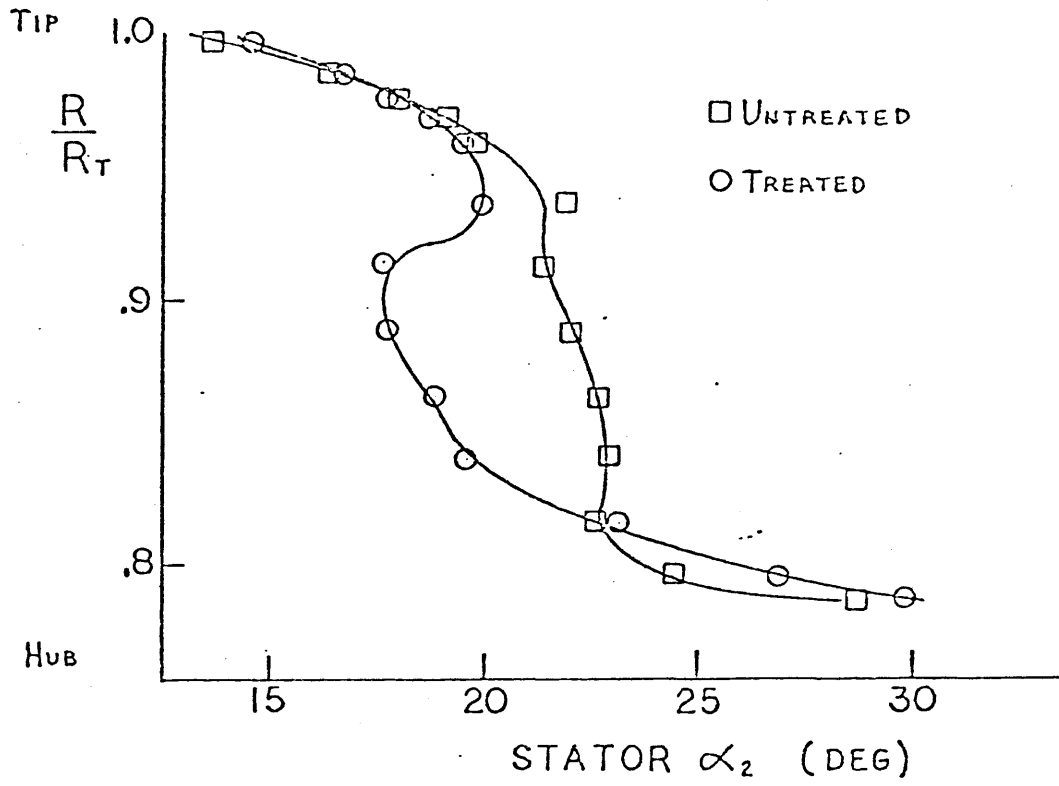


FIG. 26 UNTREATED HUB: STATOR WAKE TOTAL PRESSURE TRAVERSE, STALL POINT VS.  $\phi$  MAX, IM = .5

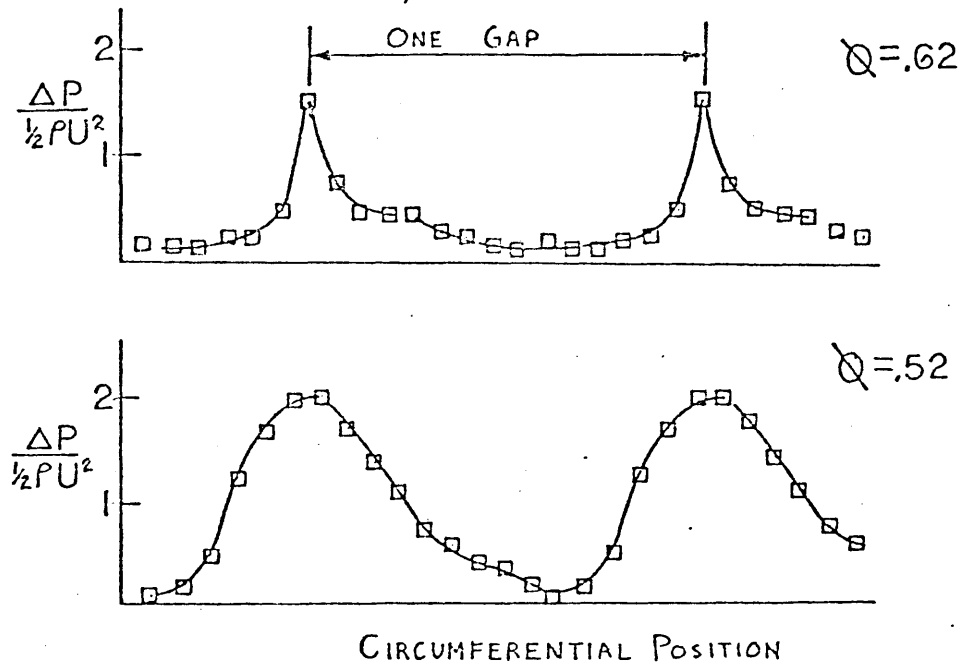


FIG. 27 UNTREATED HUB: STATOR WAKE DEVIATION ANGLE TRAVERSE, STALL POINT VS.  $\phi$  MAX, IM = .5

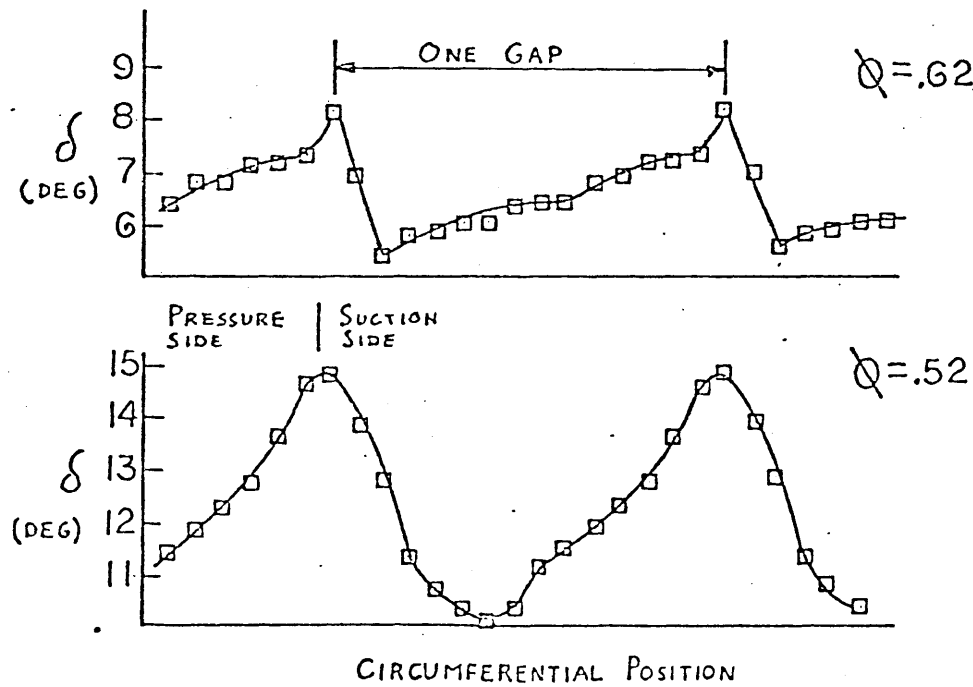




FIG. 28 TREATED HUB: STATOR WAKE TOTAL PRESSURE TRAVERSE AT STALL POINT

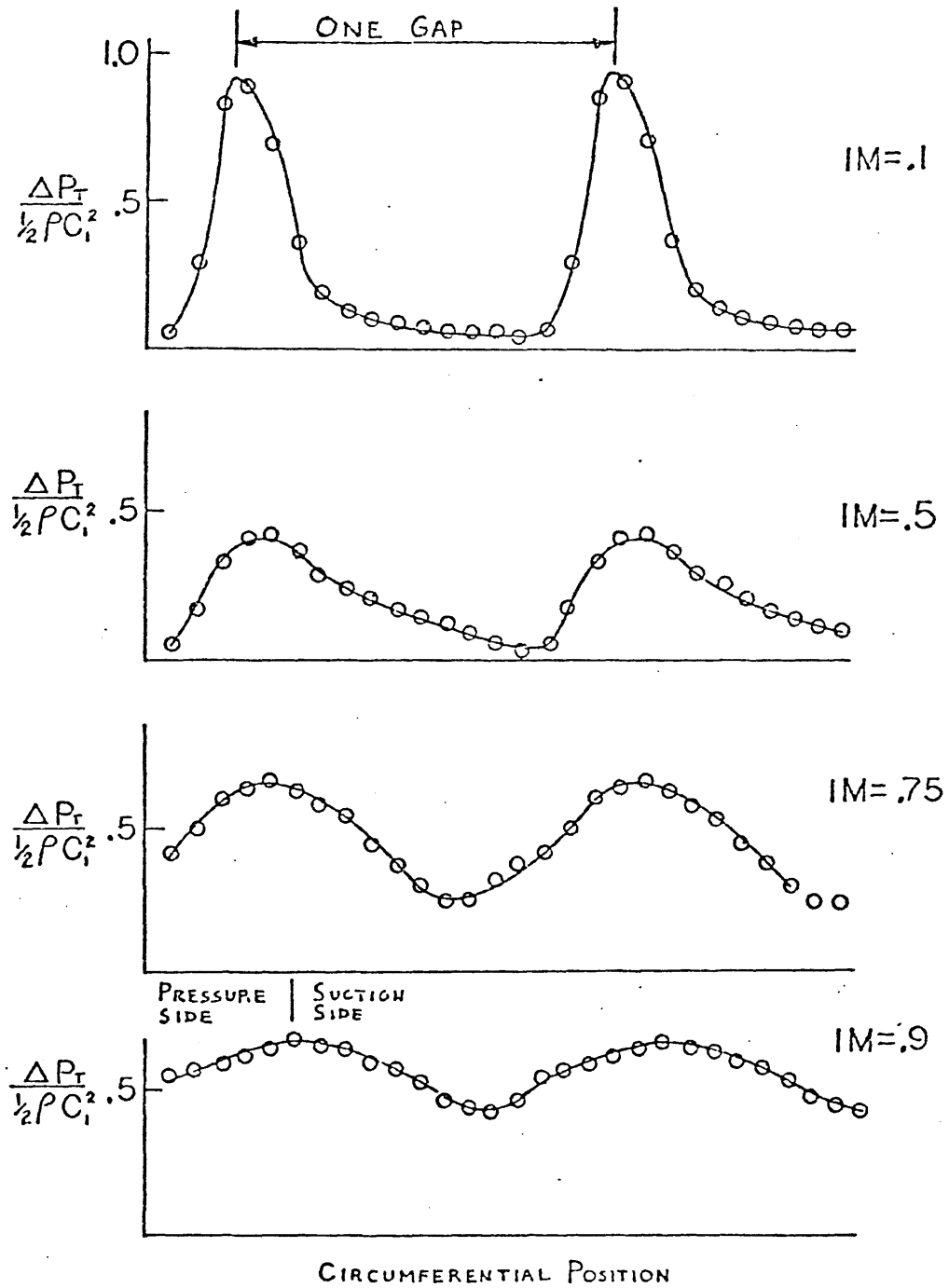


FIG. 29 UNTREATED HUB: STATOR WAKE TOTAL PRESSURE TRAVERSE AT STALL POINT

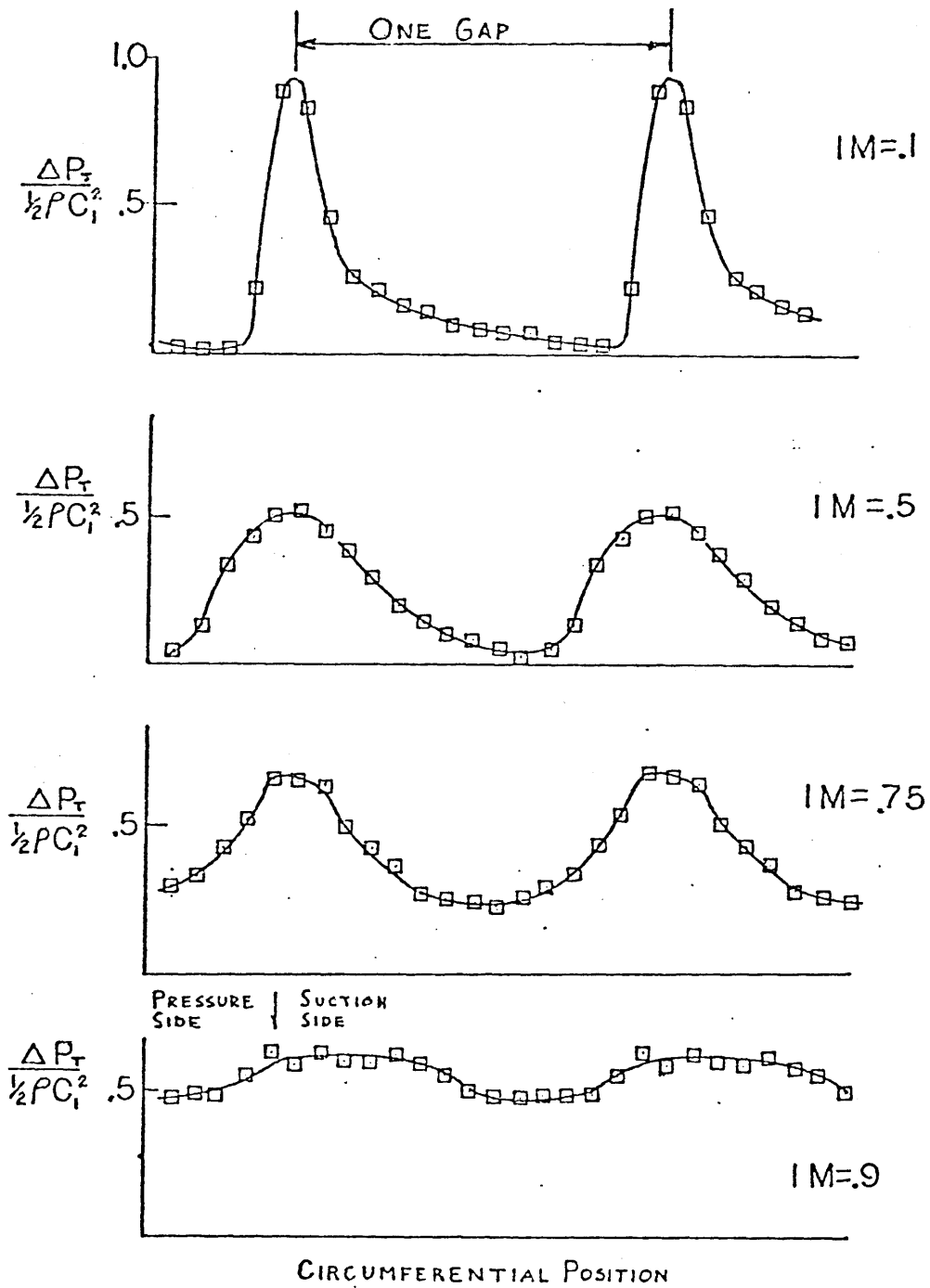


FIG. 30 TREATED HUB: STATOR WAKE DEVIATION ANGLE TRAVERSE AT STALL POINT

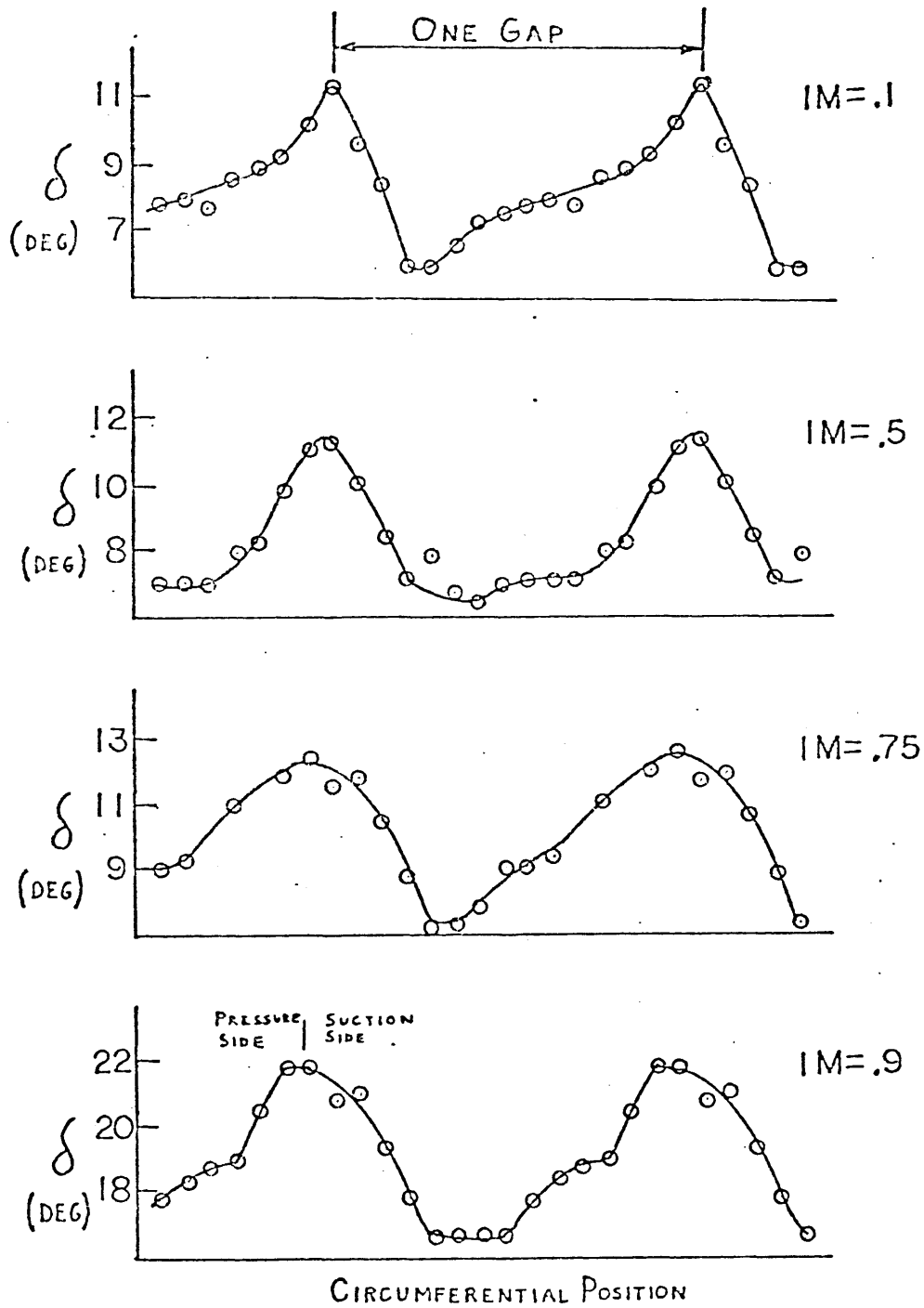


FIG. 31 UNTREATED HUB: STATOR WAKE DEVIATION ANGLE TRAVERSE AT STALL POINT

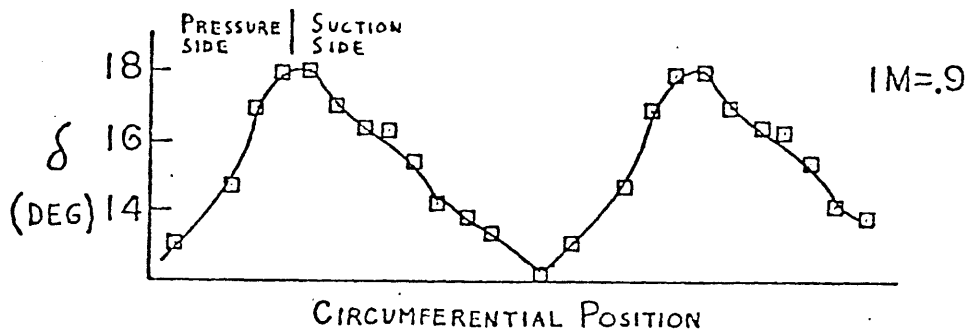
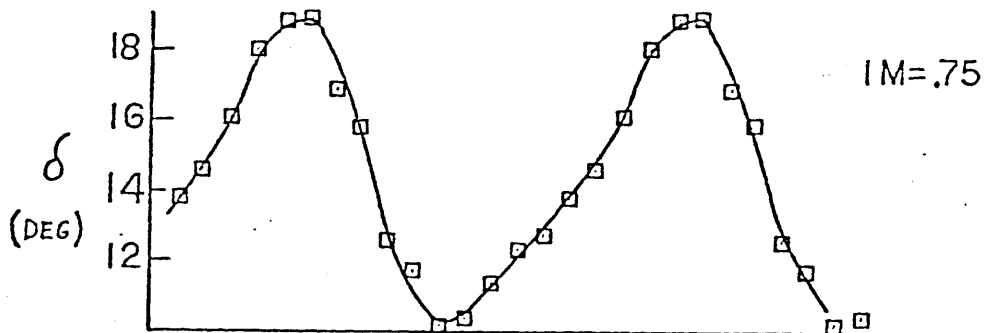
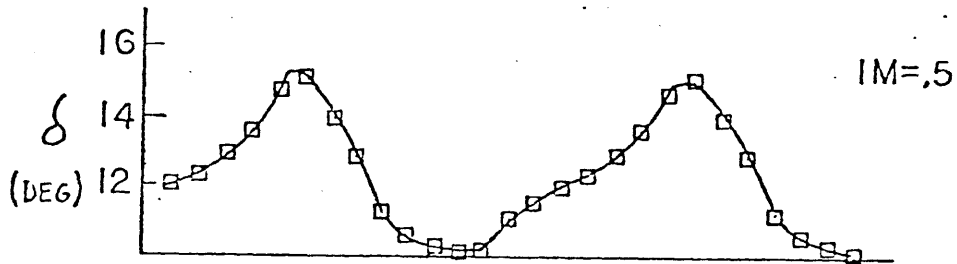
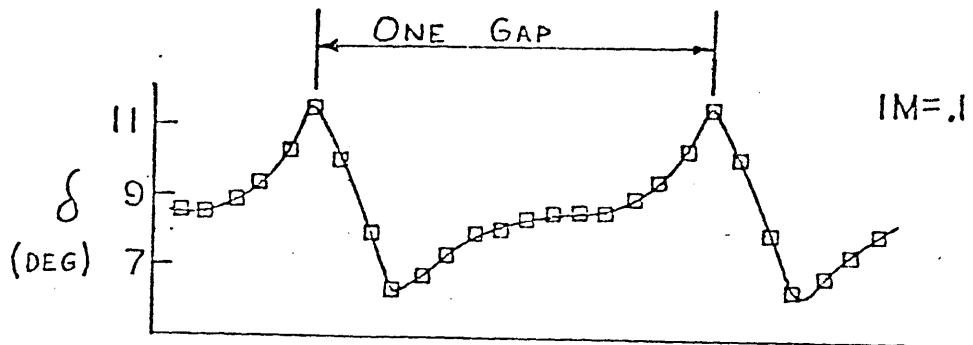


FIG. 32 UNTREATED HUB: ROTOR AND STATOR D-FACTOR PROFILES AT STALL  
(BASED ON AXISYMMETRIC CALCULATION)

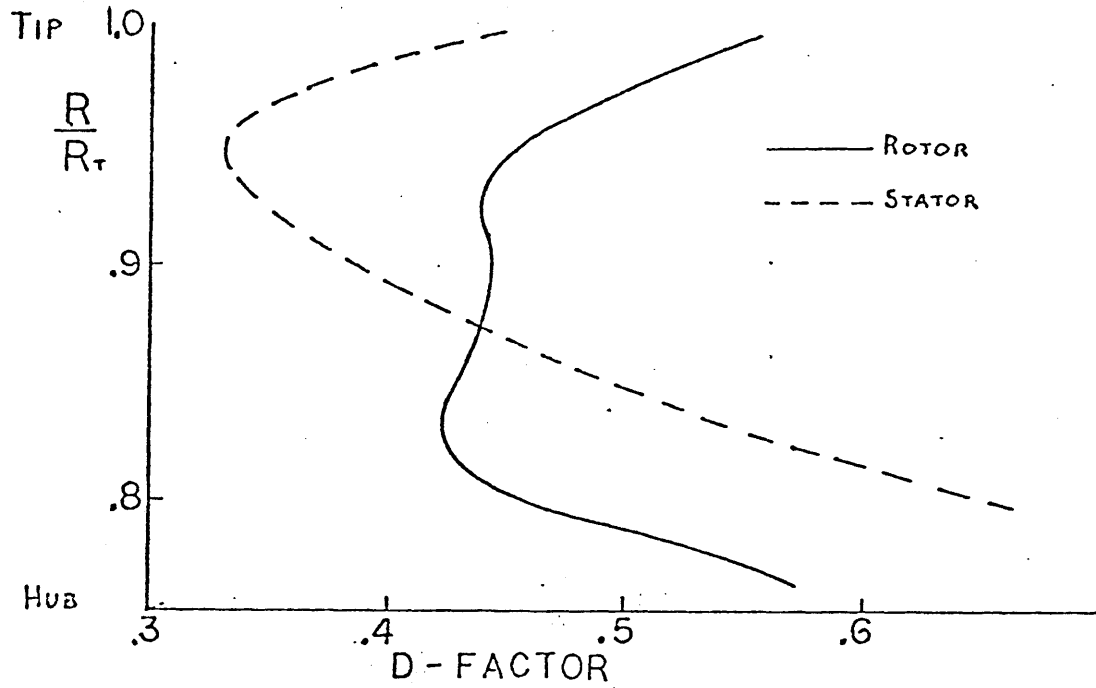


FIG. 33 UNTREATED HUB: ROTOR AND STATOR  $\Delta P/Q$  PROFILES AT STALL  
(BASED ON AXISYMMETRIC CALCULATION)

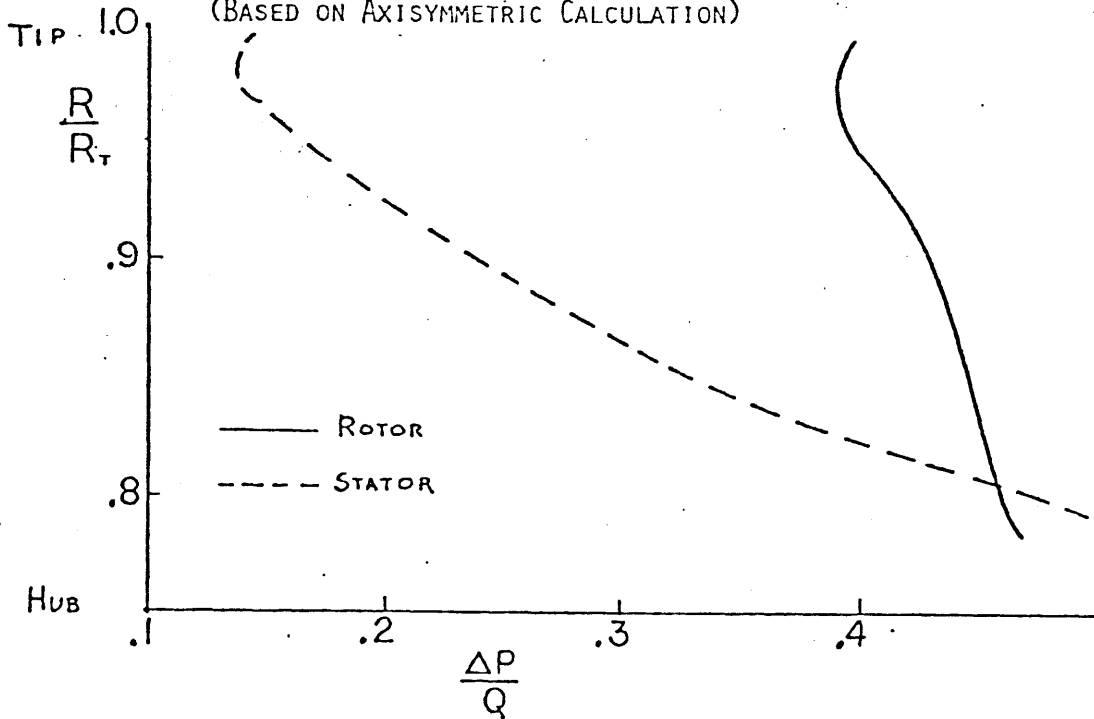


FIG. 34 STATOR D-FACTOR PROFILE AT STALL, TREATED VS. UNTREATED  
(BASED ON AXISYMMETRIC CALCULATION)

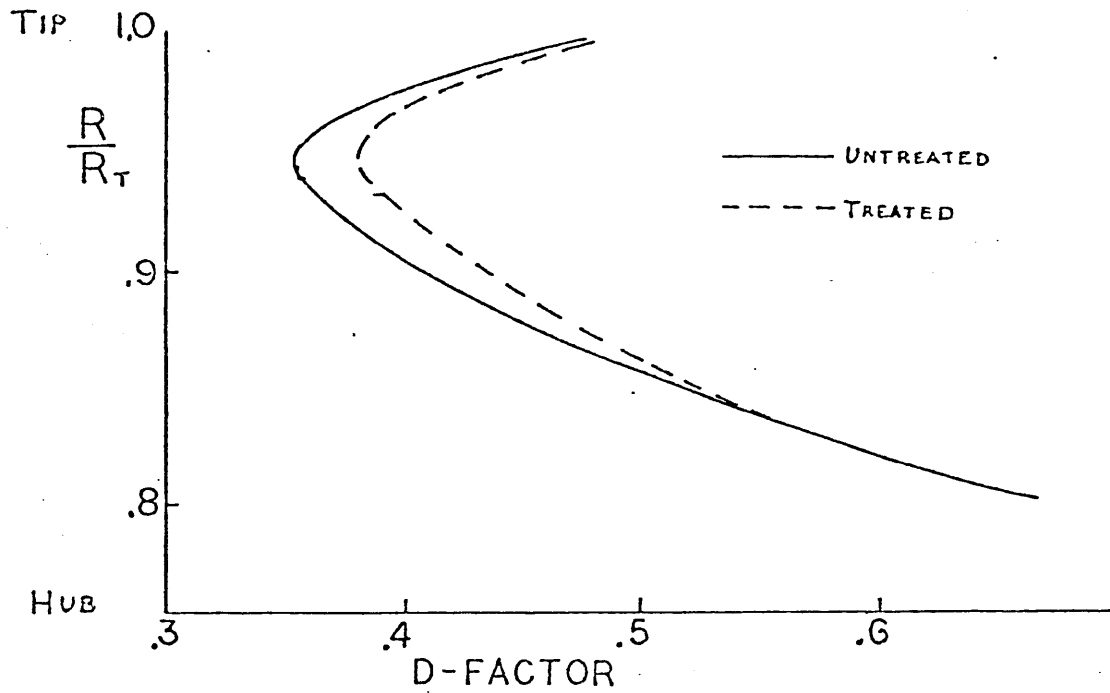


FIG. 35 STATOR  $\Delta P/q$  PROFILES AT STALL, TREATED VS. UNTREATED  
(BASED ON AXISYMMETRIC CALCULATION)

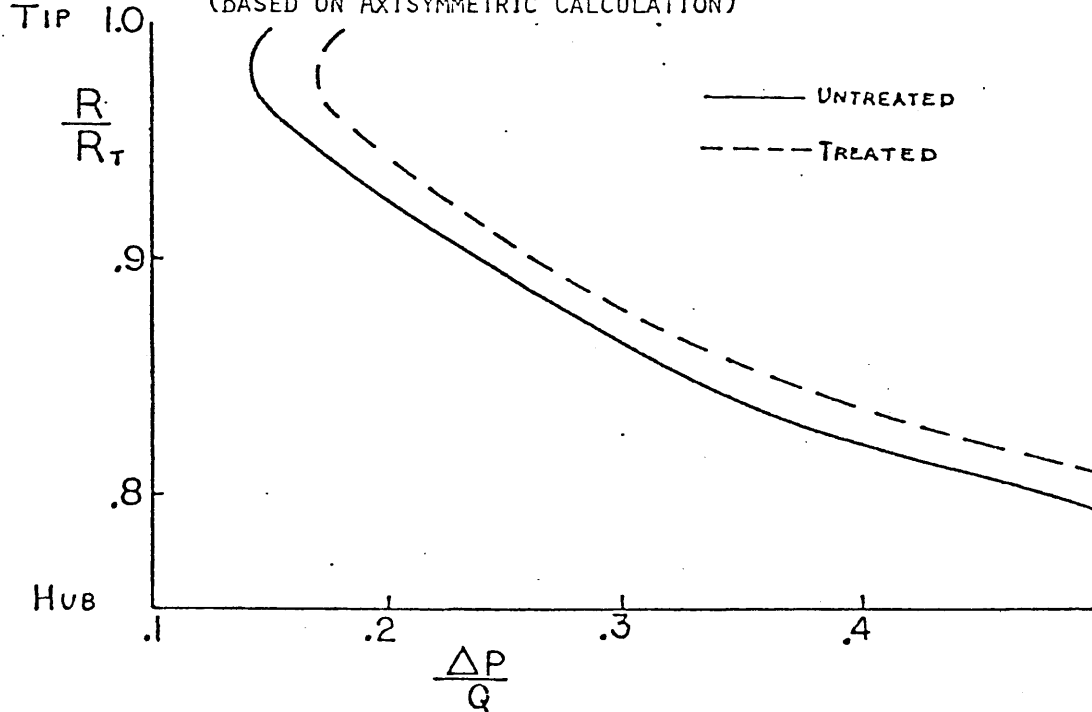


FIG. 36 STATOR AXIAL VELOCITY PROFILE AT STALL, TREATED VS. UNTREATED  
(BASED ON AXISYMMETRIC CALCULATION)

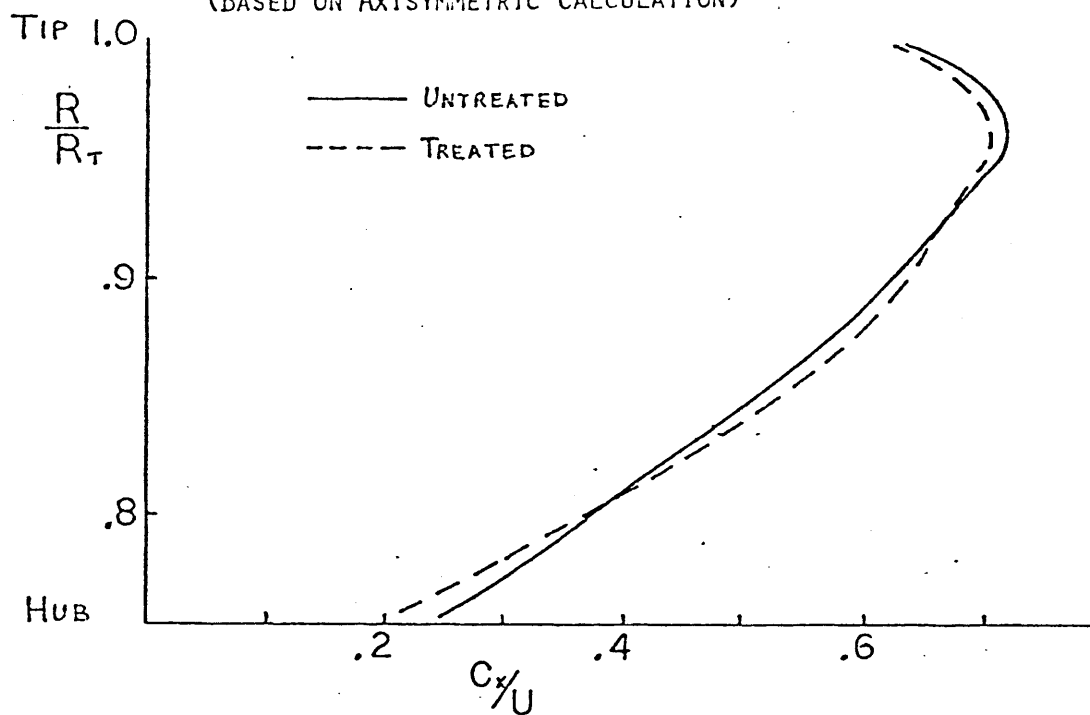


FIG. 37 STATOR RELATIVE TOTAL PRESSURE LOSS COEFFICIENT PROFILE  
AT STALL, TREATED VS. UNTREATED  
(BASED ON AXISYMMETRIC CALCULATION)

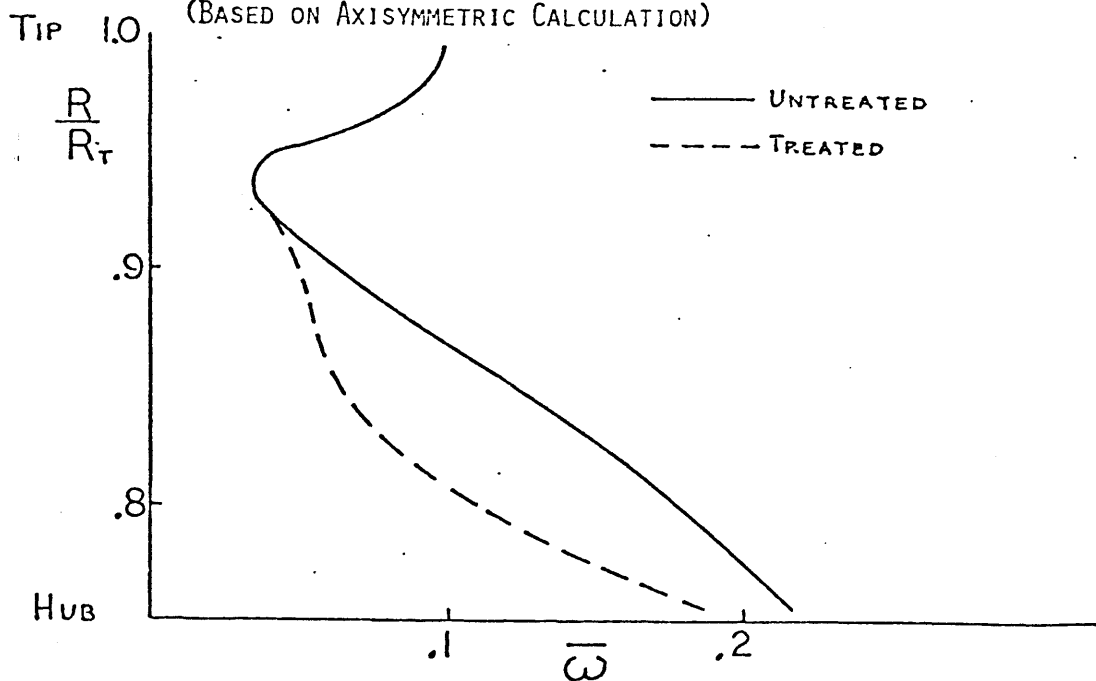
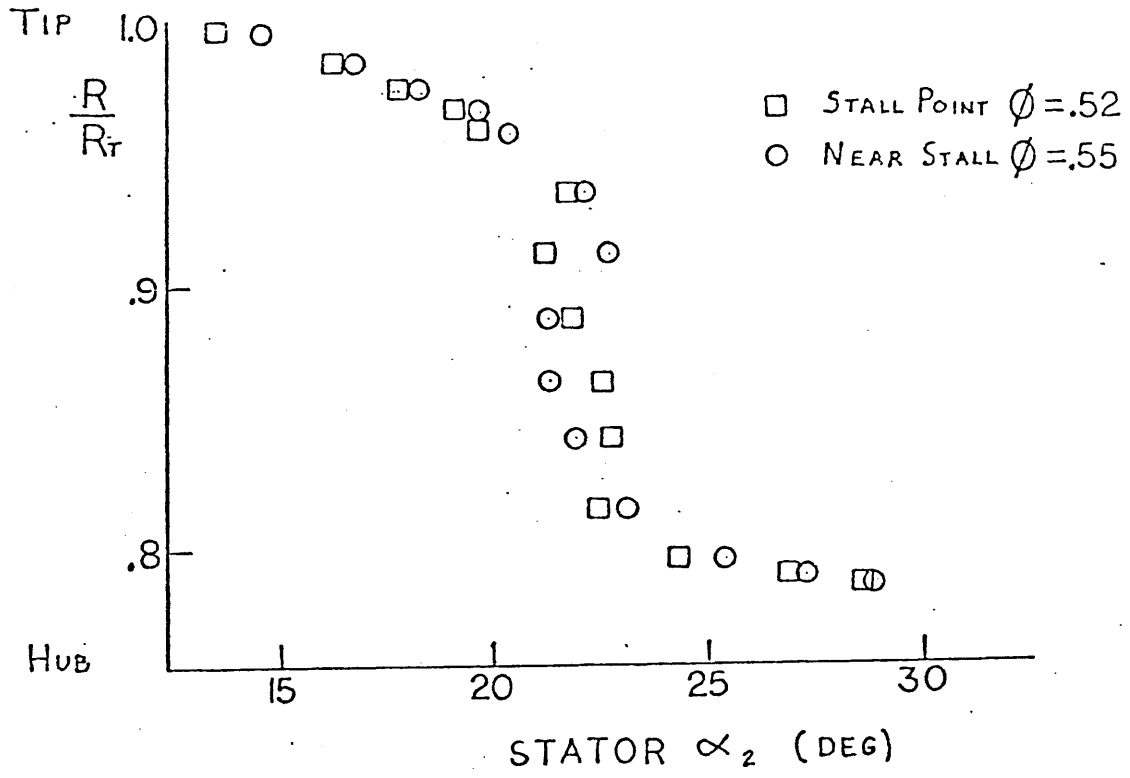
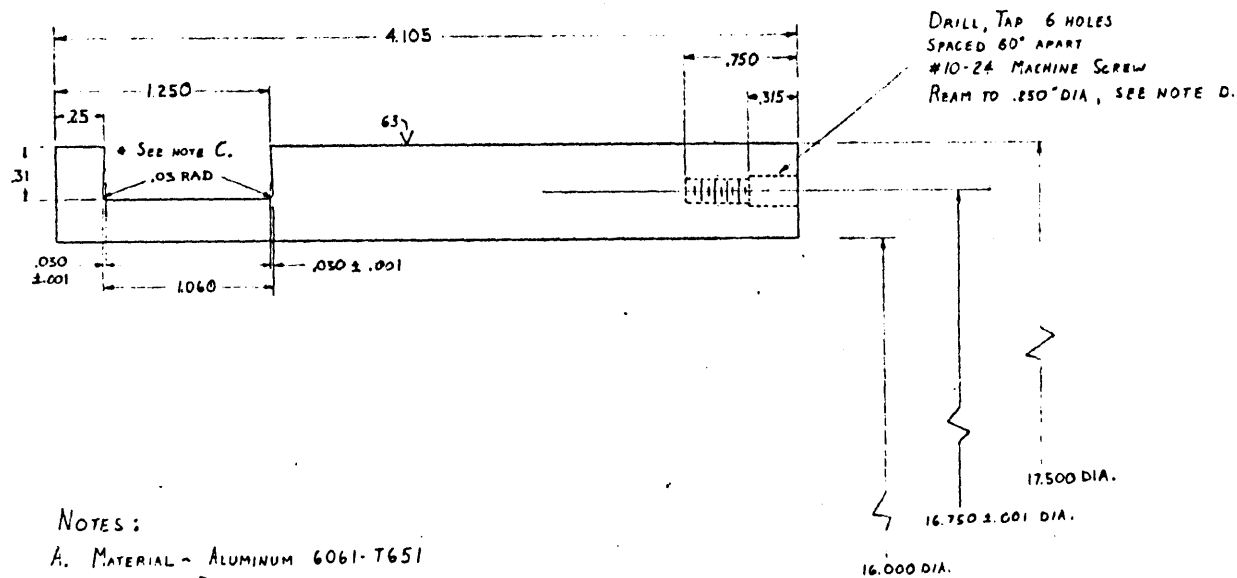


FIG. 38 UNTREATED STATOR EXIT AIR ANGLE PROFILES; STALL POINT AND "NEAR STALL" POINT







NOTES:

- A. MATERIAL - ALUMINUM 6061-T651
- B. 2 PIECES REQ'D
- C. OMIT DOVETAIL SLOT ON PIECE # 1  
PIECE # 2 AS PER DRAWING
- D. REAMING OF HOLES IN CYLINDER (PART A.)  
AND DISK (PART B.) TO BE DONE  
CONCURRENTLY TO INSURE ALIGNMENT AND  
CONCENTRICITY OF ASSEMBLY. BOTH CYLINDERS  
TO BE MATCH DRILLED AND .250" REAMED ON A  
16.750" BOLT CIRCLE WITHIN ±.001

NOTES (CON'T):

- E. ALL MACHINING MUST BE DONE WITH  
A MINIMUM OF STRESS BEING APPLIED TO  
THE PIECES. PREFERABLY ON A FACE PLATE  
AND NOT A JAWED CHUCK
- F. O.D. OF FINISHED RINGS TO BE CONCENTRIC  
WITH THE 2.25" BORE WITHIN .005 T.I.R.  
WHEN ASSEMBLED.

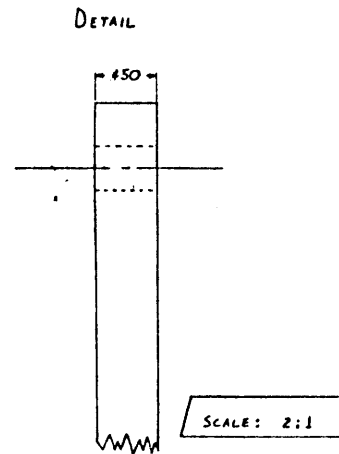
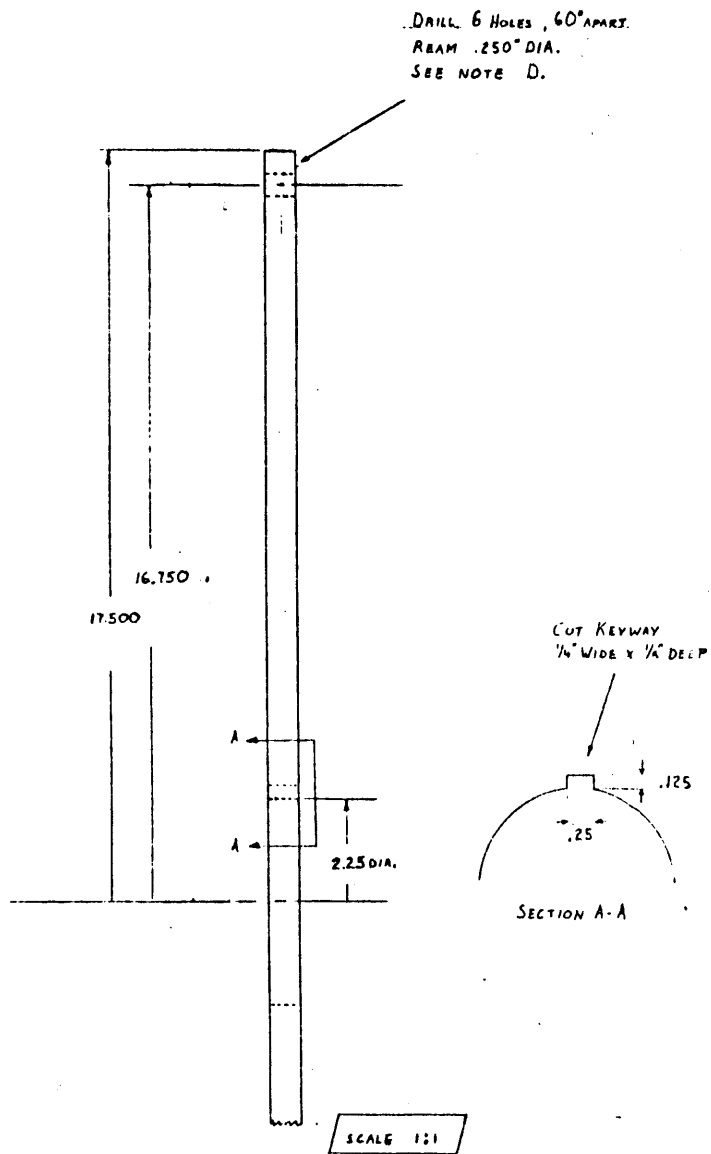
HUB TREATMENT  
CYLINDER (PART A.)

SCALE: 2X (APPROXIMATE)

TOLERANCES: .XXX - ±.005 (EXCEPT WHERE  
NOTE: .XX - ±.01)

5/14/30 II

APPENDIX A. AFT ROTOR DISK

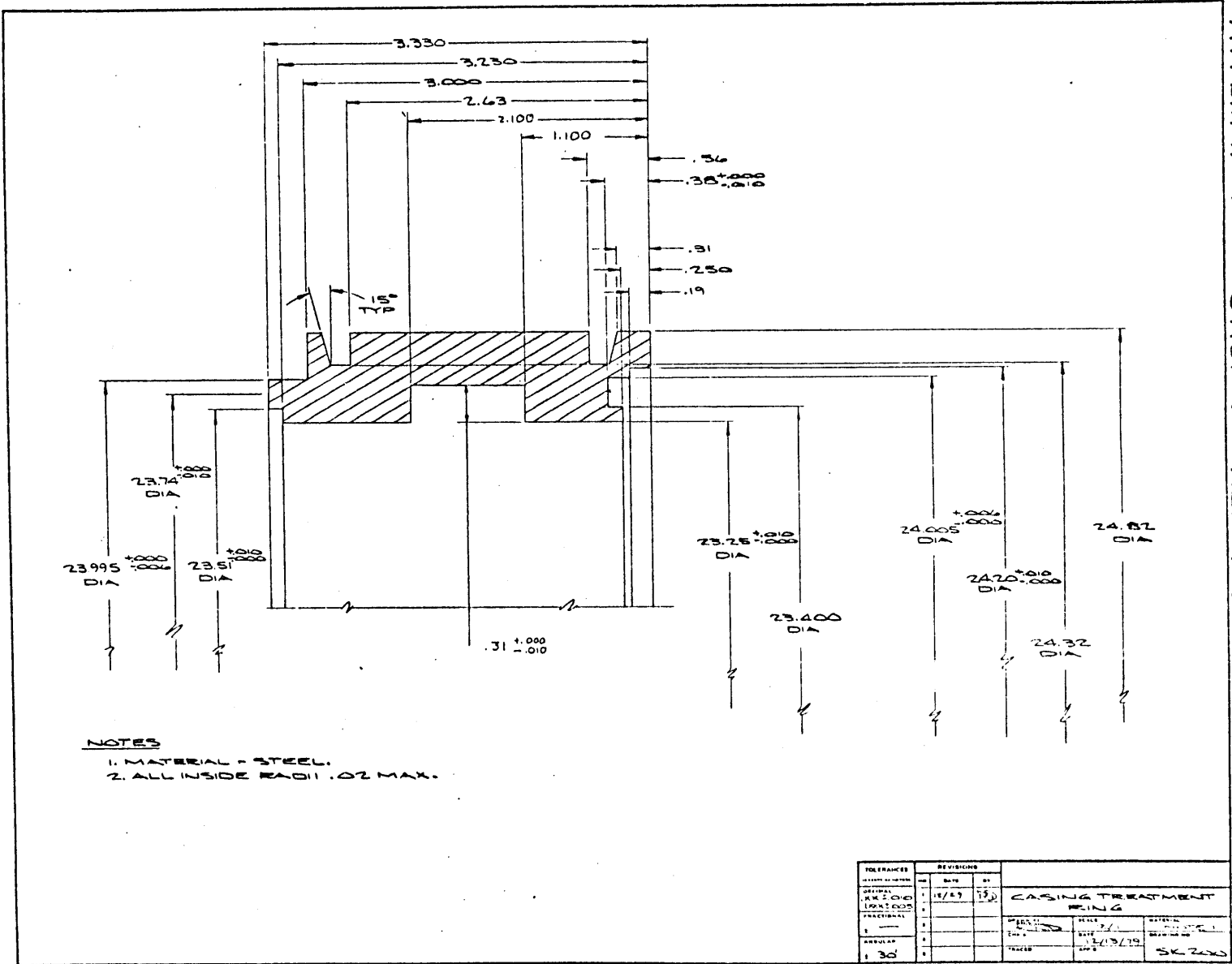


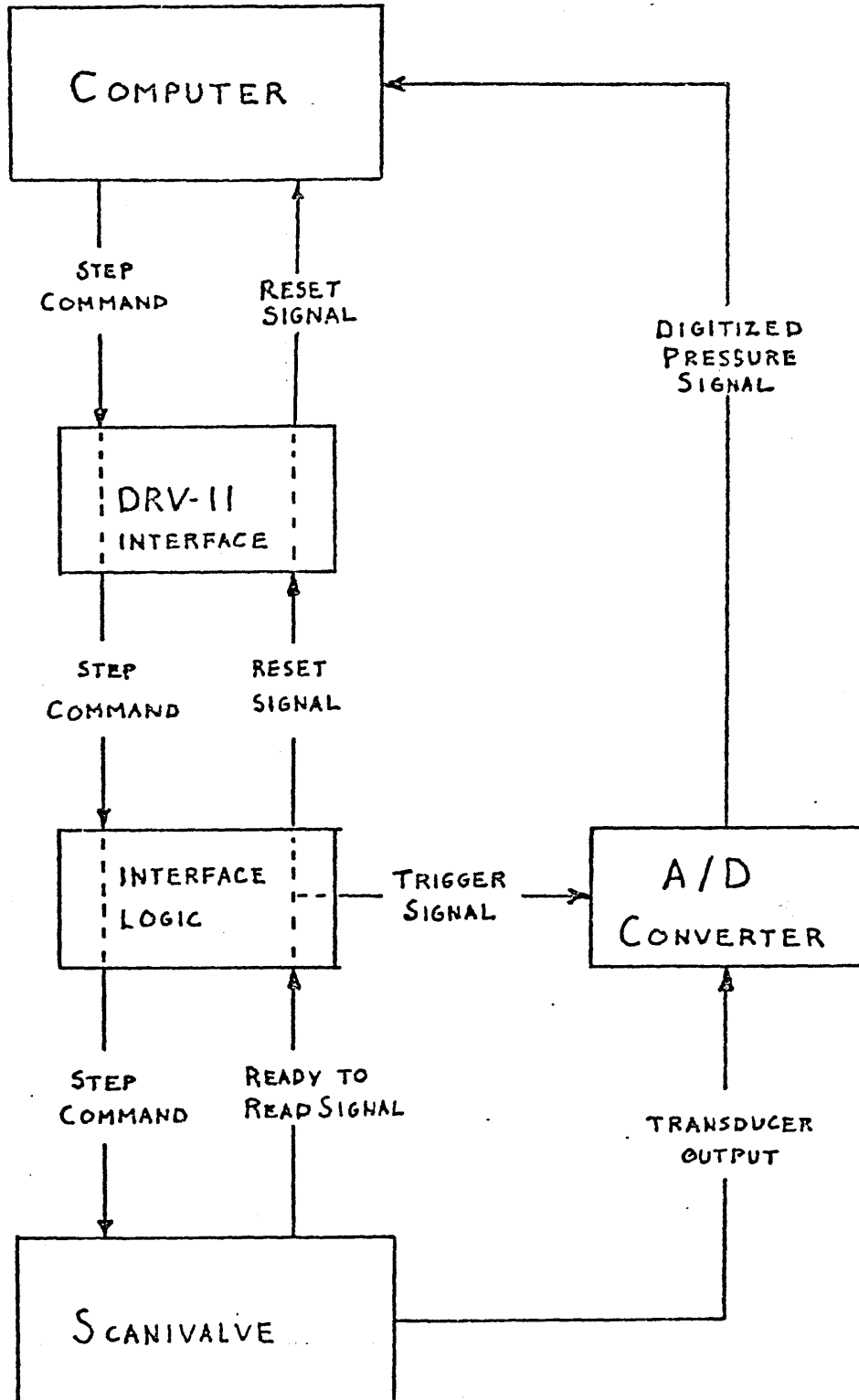
ROTOR DISK (PART B.)  
 FOR HUB TREATMENT CYLINDER

TOLERANCES .XX - ±.005  
 .XX - ±.01

MATERIAL: ALUMINUM 7075-T6

APPENDIX A. CASING TREATMENT



APPENDIX B. AUTOMATIC DATA ACQUISITION SYSTEM  
BLOCK DIAGRAM

## APPENDIX B. SCANIVALVE PROGRAM

```

C THIS PROGRAM AUTOMATICALLY STEPS THE SCANIVALVE THROUGH
C ALL 48 CHANNELS, AND RECORDS THE TRANSDUCER OUTPUT AND
C VALVE POSITION FOR EACH PORT. INITIAL INPUT IS DATE AND
C AMBIENT PRESSURE. AND FOR EACH POINT AMBIENT TEMPERATURE
C TIME. AND RPM IS INPUT. THE OUTPUT INCLUDES A LIST OF
C PRESSURES FOR EACH DATA POINT, AND CX/U AS CALCULATED BY
C THE INLET STATIC PRESSURES (CHANNELS 1-4).
      DIMENSION PT2(60)
      DIMENSION DAT(48,60)
      DIMENSION QIN(60)
      DIMENSION ADATA(48)
      DIMENSION PT4(60)
      DIMENSION PST4(60)
      DIMENSION PST5(60)
      DIMENSION PSH5(60)
      DIMENSION PTS(60)
      DIMENSION TEM(60)
      DIMENSION PRS(60)
      DIMENSION RP(60)
      DIMENSION FLOCOF(60)
      DIMENSION ICH(48)
      DIMENSION ITIME(60)
      IM=0
      NN=0
      TYPE*, 'ENTER DATE'
      ACCEPT 5, IDATE
5      FORMAT(I4)
      TYPE*, 'ENTER AMBIENT PRESS, PSIA'
      ACCEPT 6, AMPR
6      FORMAT(F6.2)
      NN=NN+1
10     IM=1
      TYPE*, 'ENTER TIME'
      ACCEPT 12, ITIM
12     FORMAT(I4)
      ITIME(NN)=ITIM
      TYPE*, 'ENTER AMBIENT TEMP, DEG C'
      ACCEPT 13, TEMP
13     FORMAT(F6.2)
      TEM(NN)=TEMP
      PRS(NN)=AMPR
      PRS(NN)=AMPR
      DO 14 J=1,48
14     ADATA(J)=0.0
      DO 20 I=1,48
      CALL DATA(KL, IPOS, ID1, ID2, ID3, ID4, ID5, ID6, ID7, ID8, ID9, ID10)
      CALL CHANCON(IPOS, ICH(I))
      XDATA=ID1+ID2+ID3+ID4+ID5+ID6+ID7+ID8+ID9+ID10
      XDATA=XDATA/10.
      XDATA=(XDATA-2048)
      ICH(I)=ICH(I)
      XDATA=2.5*XDATA/214E
      XDATA=XDATA*.375
20     DAT(I, NN)=XDATA
25     CONTINUE

```

## APPENDIX B. SCANIVALVE PROGRAM (PAGE 2)

```

1. DAT(J, NN), ICH(J+1), DAT((J+1), NN)
35  FORMAT( 13, 3X, F6.3, 5X, 12, 3X, F6.3, 5X, 12, 3X, F6.3, 5X, 12, 3X, F6.3)
30  CONTINUE
    TYPE*, ' TYPE 1 FOR FLOW CALC'
    ACCEPT 40, II
40  FORMAT(11)
    FLOCOF(NN)=0.0
    IF(II.EQ.0) GO TO 50
    PT=0.0
    PS=0.0
    DO 45 L=1, 4
    PS=PS+DAT(L, NN)
45  PT=PT+DAT((L+8), NN)
    PT=PT-DAT(9, NN)
    PT=PT/7.0
    PS=PS/4.0
    PT2(NN)=PT
    PT4(NN)=(DAT(25, NN)+DAT(27, NN)+DAT(30, NN)+DAT(32, NN))/4.0
    PST4(NN)=(DAT(33, NN)+DAT(34, NN)+DAT(35, NN)+DAT(36, NN))/4.0
    PST5(NN)=(DAT(41, NN)+DAT(42, NN)+DAT(43, NN)+DAT(44, NN))/4.0
    PSH5(NN)=(DAT(45, NN)+DAT(46, NN)+DAT(47, NN)+DAT(48, NN))/4.0
    PTS(NN)=(DAT(37, NN)+DAT(38, NN)+DAT(39, NN)+DAT(40, NN))/4.0

    TYPE*, ' ENTER RPM'
    ACCEPT 46, RPM
46  FORMAT(F8.2)
    RP(NN)=RPM
    TEMP=(TEMP*9.0/5.0)+32.0
    RHO=AMPR*144.0/(53.3*(460.0+TEMP))
    V=((3273.6/RHO)*((-0.012)-PS))*0.5
    QIN(NN)=(V**2.0)*RHO/(32.2*2.0+144)
    SPD=RPM*.0889
    CZU=V/SPD
    FLOCOF(NN)=CZU
    TYPE*, ' CZU=' , CZU
50  TYPE*, ' TYPE 1 TO CONTINUE, 0 TO STOP'
    ACCEPT 55, JJ
55  FORMAT(11)
    IF(JJ.EQ.0) GO TO 56
    IF(NN.GT.59) GO TO 56
    GO TO 10
    MM=1
56  CONTINUE
    DO 75 M=1, NN
    PRINT*, ' DATA POINT#', M
    PRINT*, ' TIME=' , ITIME(M), ' DATE=' , IDATE
    PRINT*, ' AMBIENT TEMP=' , TCM(M)
    PRINT*, ' AMBIENT PRESS=' , PRS(M)
    PRINT*, ' RPM=' , RP(M)
    PRINT*, ' STA 2 PITCH TOT. PRESS=' , PT2(M)
    PRINT*, ' STA 4 PITCH TOT. PRESS=' , PT4(M)
    PRINT*, ' STA 4 CASE STAT. PRESS=' , PST4(M)
    PRINT*, ' STA 5 PITCH TOT. PRESS=' , PTS(M)
    PRINT*, ' STA 5 CASE STAT. PRESS=' , PST5(M)
    PRINT*, ' STA 5 HUB STAT. PRESS=' , PSH5(M)
    DO 60 L=3, 47, 4
    PRINT 65, ICH(L-2), DAT((L-2), M), ICH(L-1), DAT((L-1), M), ICH(L)
    1. DAT(L, M), ICH(L+1), DAT((L+1), M)

```

## APPENDIX B. SCANIVALVE PROGRAM (PAGE 3)

```
65      FORMAT( 13,3X,F6.3,5X,12,3X,F6.3,5X,12,3X,F6.3,5X,12,3X,F6.3)
60      CONTINUE
        PRINT*,' INLET "Q"=' ,QIN(M)
        PRINT*,' FLOW COEFFICIENT=' ,FLOCOF(M)
        PRINT 61,
61      FORMAT(' 0' )
62      CONTINUE
        IF(IM.EQ.1) GO TO 72
70      CONTINUE
        IM=1
        PRINT 71,
71      FORMAT(' 1' )
        GO TO 75
72      IM=0
75      CONTINUE
        STOP
        END
```

## APPENDIX B. SUBROUTINES FOR SCANIVALVE PROGRAM

C THIS SUBROUTINE PROVIDES THE SOFTWARE FOR THE DIGITAL  
 C OPERATION OF THE SCANIVALVE THROUGH DRV11 INTERFACE.  
 C THE SCANIVALVE IS STEPPED, TRANSDUCER VOLTAGE READ 10  
 C TIMES, AND CHANNEL CODE RECORDED FOR EACH VALVE POSITION.

```
.GLOBL DATA
DATA:  MOV (RS)+,R0
      CLR @#171770
      MOV @#(RS)+,@#171772
ADDRES: TST @#171770
      BPL ADDRES
      MOV @#171774,@#(RS)+
      CLR R1
READ:   CLR @#170400
      MOV #200,@#170402
PRS:   TST @#170400
      BPL PRS
      MOV @#170402,@#(RS)+
      INC R1
      CMP #12,R1
      BPL READ
      RTS PC
      .END DATA
```

C THIS SUBROUTINE CONVERTS THE DIGITAL CHANNEL CODE FROM  
 C THE SCANIVALVE INTO THE APPROPRIATE CHANNEL NO.

```
SUBROUTINE CHANCON(IPOS,ICHN)
IF(IPOS.LT.10) GO TO 40
IF(IPOS.GT.30) GO TO 10
ICHN=IPOS-6
GO TO 50
10 IF(IPOS.GT.42) GO TO 20
ICHN=IPOS-12
GO TO 50
20 IF(IPOS.GT.60) GO TO 30
ICHN=IPOS-18
GO TO 50
30 ICHN=IPOS-24
GO TO 50
40 ICHN=IPOS
50 CONTINUE
RETURN
END
```



## APPENDIX C. HOT WIRE DIGITIZING PROGRAM

```

;THIS PROGRAM ENABLES THE DATL LSI-2 A-D CONVERTER AND DMA TO DIGITIZE
;THE ANALOG SIGNALS AT ITS 16 CHANNELS IN AUTOINCREMENT,EXTERNAL TRIGGERED
;POLLING MODE. A MAXIMUM OF 125 BLOCKS OF DATA CAN BE ACHIEVED AND WRITTEN
;ON FLOPPY DISK WITH FILE NAME FLOW.
;

```

```

.TITLE ACQUIRE DATA IN POLLING MODE.
.MCALL .WRITW,.ENTER,.CLOSE,.EXIT
S1:   RESET
      MOV #START,R1
      MOV #FINAL,R2
      MOV R1,R0
      MOV #3002,@#170400
DLOOP: TST @#170400
       BPL DLOOP
       MOV @#170402,(R0)+
       CMP R2,R0
       BGE DLOOP
S2:   MOV #AREA,R4           ;EMT ARGUMENT.
      CLR R3                ;OUTPUT CHANNEL=0.
      WCNT=200              ;NO. OF WORDS=200.
      WCNT2=WCNT*2          ;BYTE NO.=400.
      ENDW=FINAL-WCNT2+2    ;
      CLR R5                ;BLOCK COUNT.
      .ENTER R4,R3,#DYNAM,#-1 ;CREATE FILE.
WLOOP: .WRITW R4,R3,R1,#WCNT,R5;WRITE THAT BLOCK.
       ADD #WCNT2,R1        ;R1 POINTS TO
                           ;NEXT WORD.
       INC R5               ;UPDATE BLOCK NO..
       CMP #ENDW,R1        ;
       BGE WLOOP           ;COMPLETE?
       .CLOSE R3           ;
       .EXIT               ;
DYNAM: .RADS0/DY1/         ;PHYSICAL DEVICE.
       .RADS0/FLOW DAT/    ;FILENAME AND TYPE.
AREA:  .BLKW 10            ;EMT ARGUMENT LIST.
START: .BLKW 76400
FINAL: .BYTE
      .END S1

```

## APPENDIX C. FFT PROGRAM

C THIS PROGRAM USES THE FFT OF THE LAB. SUBROUTINES PACKAGE TO COMPUTE  
C THE FOURIER TRANSFORM OF A DATA SEQUENCE.

```

      DIMENSION IWR(4096),IMAG(4096),NLINE(8),WR(4096)
      LOGICAL*1 IYES,YES
      DATA NLINE//DY', '1:', ' ', ' ', ' ', ' ', ' ', ' ', 'D', 'AT', ' ', ' ' /
      DATA YES//Y' /
      TYPE*, 'FORWARD OR INVERSE FOURIER TRANSFORM?'
      ACCEPT*, INURS
66      TYPE*, 'ENTER 6-CHARACTER FILENAME'
      ACCEPT 1000, (NLINE(I), I=3,5)
1000     FORMAT(3A2)
      OPEN(UNIT=8, NAME=NLINE, TYPE='OLD', FORM='UNFORMATTED')
      READ(8)IH.(IWR(I), I=1, IH)
      CLOSE(UNIT=8)
1050     FORMAT(1A1)
      DO 123 I=1, IH
123      IMAG(I)=0
      CALL FFT(IE, IH, IWR, IMAG, INURS, ISF)
      IF(IE)99, 2, 99
2        IF(ISF.NE.0)TYPE 999, ISF
      DO 987 I=1, 4096
      A=IWR(I)
      A=A**2
      WR(I)=IMAG(I)
      WR(I)=WR(I)**2
      WR(I)=(A+WR(I))
987      WR(I)=(WR(I))**.5
      TYPE*, 'ENTER FILENAME FOR TRANSFORMED DATA'
      ACCEPT 1000, (NLINE(I), I=3,5)
      OPEN(UNIT=9, NAME=NLINE, TYPE='NEW', FORM='UNFORMATTED')
      WRITE(9)IH.(WR(I), I=1, IH), (IMAG(I), I=1, IH)
      CLOSE(UNIT=9)
999      FORMAT(///, 1X, 'THE SCALE FACTOR RETURNED IS', I4)
99      TYPE 998, IE
998      FORMAT(///, 1X, 'THE ERROR CODE RETURNED=', I4)
      TYPE*, 'ANYMORE DATA SET TO GO?'
      ACCEPT 1050, IYES
      IF(IYES.EQ.YES) GO TO 99
      END

```